$$a\theta = a\int_t^{t'} x\,dt + \frac{k_n}{k_{11}}\int_t^{t'} x^{n-1}\,dt + \frac{k_n}{k_1}\int_t^{t'} x^n dt = \frac{1}{k_{11}}(\ln x_t - \ln x_{t'}) + \frac{1}{k_1}(x_t - x_{t'}) \quad (22)$$

$$\frac{a\theta}{x_t - x_{t'}} + \frac{a\int_t^{t'} x\,dt}{x_t - x_{t'}} + \frac{k_n\int_t^{t'} x^{n-1}\,dt}{k_{11}(x_t - x_{t'})} + \frac{k_n\int_t^{t'} x^n\,dt}{k_1(x_t - x_{t'})} = \frac{1}{k_1} + \frac{1}{k_{11}}\frac{\ln x_t - \ln x_{t'}}{x_t - x_{t'}} \quad (23)$$

each member by $(x_t - x_{t'})$. A comparison with eq 6 shows that this equation contains three correcting terms in which the implicit integrals can be calculated numerically from the experimental curve by using the trapezoidal method. However, since two of these terms include the unknown constants k_1 and k_{11}, an iterative calculation process must be applied. To initiate this iterative process, a first set of k_1 and k_{11} values was obtained by neglecting the two terms containing k_1 and k_{11}. Subsequently, calculations were performed by correcting the left-hand term and by applying a test of convergence of 0.2% to k_1 and k_{11}. The blank reaction parameters, n and k_n, were determined before each series of runs (n was usually lying between 0.7 and 1.0) and a was estimated from the initial ketone concentration and from the amount of halogen which had reacted with the ketone. All results obtained by using these corrections never deviated more than 10% from uncorrected ones.

We usually prformed several runs on the same ketone and halide solution at different halogen concentrations. We then had to correct halide and ketone concentrations from one run to the next by considering the formation of α-iodo or α-bromo ketone. We then assumed that the halogeno compounds are much less reactive, as was previously observed.[77]

Supplementary Material Available: Tables S1, S2, S3, and S4 of primary kinetic data (10 pages). Ordering information is given on any current masthead page.

(77) Watson, H. B.; Yates, E. D. *J. Chem. Soc.* **1932**, 1207–1215.

Formation of Stable Bilayer Assemblies in Water from Single-Chain Amphiphiles. Relationship between the Amphiphile Structure and the Aggregate Morphology

Toyoki Kunitake,* Yoshio Okahata, Masatsugu Shimomura, Sho-ichiro Yasunami, and Kunihide Takarabe

Contribution No. 613 from the Department of Organic Synthesis, Faculty of Engineering, Kyushu University, Fukuoka 812, Japan. *Received March 31, 1981*

Abstract: The aggregate morphology of 62 single-chain amphiphiles prepared in these laboratories was examined by electron microscopy, and the relationship between the structural elements of the amphiphile and the aggregate morphology was discussed. The aggregate morphology includes globules, multi-, and single-walled vesicles, rods, tubes, and disks. Some of the morphologies are designed as pre-lamella, pre-rod, pre-disk, etc., because of their incomplete assemblage. The basic building block of these morphologies is the bilayer assembly. The structural elements of the amphiphile are conveniently divided into (1) flexible tail, (2) rigid segment, (3) hydrophilic head group, (4) spacer group, and (5) additional interacting group. The first three elements are essential for stable self-assembly, but all five elements affect the aggregate morphology. The flexible tail is linear methylene chains (or their related structures) of C_7 or longer. The rigid segment usually consists of two benzene rings (biphenyl, diphenylazomethine, azobenzene, etc.) and affects the aggregate morphology by its dipolar property and geometry (conformation). The bilayer formation is promoted by dipolar rigid segments and the high-curvature aggregate (rods and tubes) results from bent rigid segments. The disk-shaped aggregate can be obtained from a combination of the extended and bent conformations of a rigid segment. This is supported separately by the morphology change of a two-component system which contains the extended and bent rigid segments. Among the hydrophilic head groups used (trimethylammonium, modified ammonium, phosphate, sulfonate, phosphocholine, and poly(oxyethylene)), the trimethylammonium group appears to be least effective for the molecular alignment. The spacer group is the methylene chain inserted between the rigid segment and the head group. Longer spacers (usually C_{10}) yield well-defined aggregates more effectively than the shorter ones. A most notable example of the additional interacting group is given by the ester group at the tail end, which transforms globular aggregates into vesicles. The aggregation behavior other than the morphology was studied for typical ammonium amphiphiles with different rigid segments. Finally, the light-induced dynamic control of the aggregate morphology was discussed in relation to the static control based on the amphiphile structure. The temperature dependence of the fluorescence intensity of the biphenyl rigid segment was shown to depend on the aggregate morphology.

The biological cell contains many kinds of organelles such as nucleus, mitochondria, ribosome, and the Golgi apparatus. These organelles have characteristic morphologies that are directly related to the respective biological functions.[1] The organelles are self-assembling systems which are composed mostly of proteins and biomembranes. The importance of morphology in relation to the function is obvious in the biological world; however, the morphology-related function is virtually nonexistent in chemistry. If synthetic, self-assembling systems which possess designed morphologies can be developed, a totally new field of chemistry may emerge.

The present study is our initial attempt to this direction. The micellar system and other aqueous aggregates have served this purpose to a certain extent; however, they are usually very fluid and cannot have fixed morphologies.[2] It has been shown since 1977[3,4] that a variety of single-chain and double-chain amphiphiles

(1) E.g.: Lehninger, A. L. "Biochemistry"; Worth Publishers: New York, 1975.

(2) E.g.: (a) Fendler, J. H.; Fendler, E. J. "Catalysis in Micellar and Macromolecular Systems"; Academic Press: New York, 1975. (b) Menger, F. M. *Acc. Chem. Res.* **1979**, *12*, 111–117.

(3) Kunitake, T.; Okahata, Y. *J. Am. Chem. Soc.* **1977**, *99*, 3860–3861.

0002-7863/81/1503-5401$01.25/0

Chart I

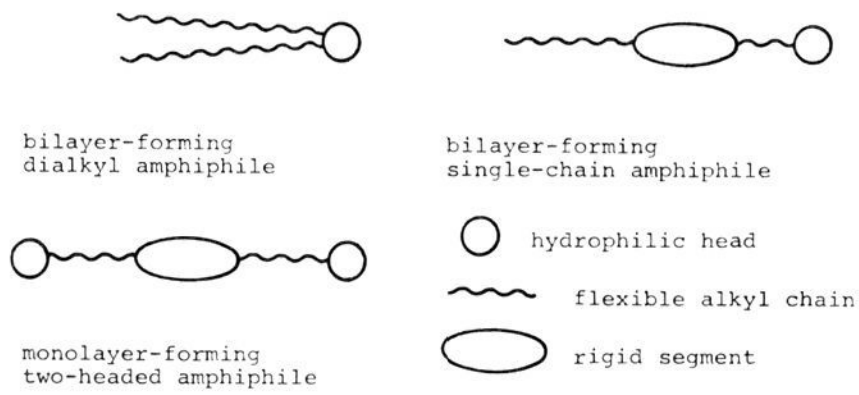

assemble spontaneously to form stable monolayers and bilayers. In the case of dialkyl (double-chain) amphiphiles, the aggregate morphology was usually vesicles and lamellae of the bilayer.[5] Similar results were obtained for bilayer-forming, single-chain amphiphiles.[6,7] On the other hand, the aggregate morphology of two-headed ammonium amphiphiles was much more varied, and tubular or rodlike aggregates were found by electron microscopy, in addition to the usual vesicles and lamellae.[8] These results imply that the aggregate morphology can be controlled by using appropriately desgined amphiphile structures. The bilayer-forming, single-chain amphiphile appears especially suitable for this purpose, because the structural variation is relatively easy. We report in this paper the self-assembling behavior of a large number of newly prepared single-chain amphiphiles. These data are combined with the related data of our previous studies, and the relationship between the amphiphile structure and the aggregate morphology is discussed.

Results and Discussion

Chemical Structures of Amphiphiles. The chemical structures of 62 amphiphiles are shown in Table I. They are all prepared in these laboratories. The basic structural features of the amphiphiles are the presence of hydrophilic head group, rigid segment, and flexible tail. The head group is in many cases the trimethylammonium group (abbreviated as N^+), but modified ammonium groups and other types (anionic, zwitterionic, and nonionic) of hydrophilic groups are included. The counteranion of the ammonium groups is invariably bromide. The flexible tail is usually normal alkyl chains (abbreviated as C_n), but the vinyl group and the ester linkage are present in some cases. A branched tail is used in one case (**13**).

The amphiphiles are divided into four major classes by the chemical structure of the rigid segment. The first class contains the diphenylazomethine unit as the rigid segment. The second and third classes contain the biphenyl unit and the azobenzene and azoxybenzene units, respectively. The fourth class contains other types of rigid segment that are composed of two (and three) benzene rings connected by various atoms or groups.

The "spacer" group is the structural unit between the head group and the rigid segment. The spacer is in most cases the linear methylene chain, but the alanyl unit is involved in three examples.

We stated in a previous publication that the liquid crystalline property is an integral part of the bilayer formation. The molecular arrangement in the monolayer and bilayer of single-chain amphiphiles is fundamentally the same as that of the smectic mesophase. According to Gray,[9] structural requirements for the mesomorphic behavior are (i) elongated molecular geometry which is rod- or lathlike in shape and (ii) appropriate intermolecular attractions for maintaining parallel molecular packing. It is expected, therefore, that the amphiphilic molecules with these structural characteristics form stable membrane assemblies in water. The compounds listed in Table I satisfy these structural requirements, since they contain long hydrocarbon chains and elongated aromatic groups (rigid segments). In fact, many of the amphiphiles and their precursers show thermotropic liquid crystalline textures during the melting point measurement. Our initial selection of the rigid segment was based on the aromatic structures which are involved in the typical liquid crystalline material, as exemplified by diphenylazomethine, biphenyl, and azobenzene units.

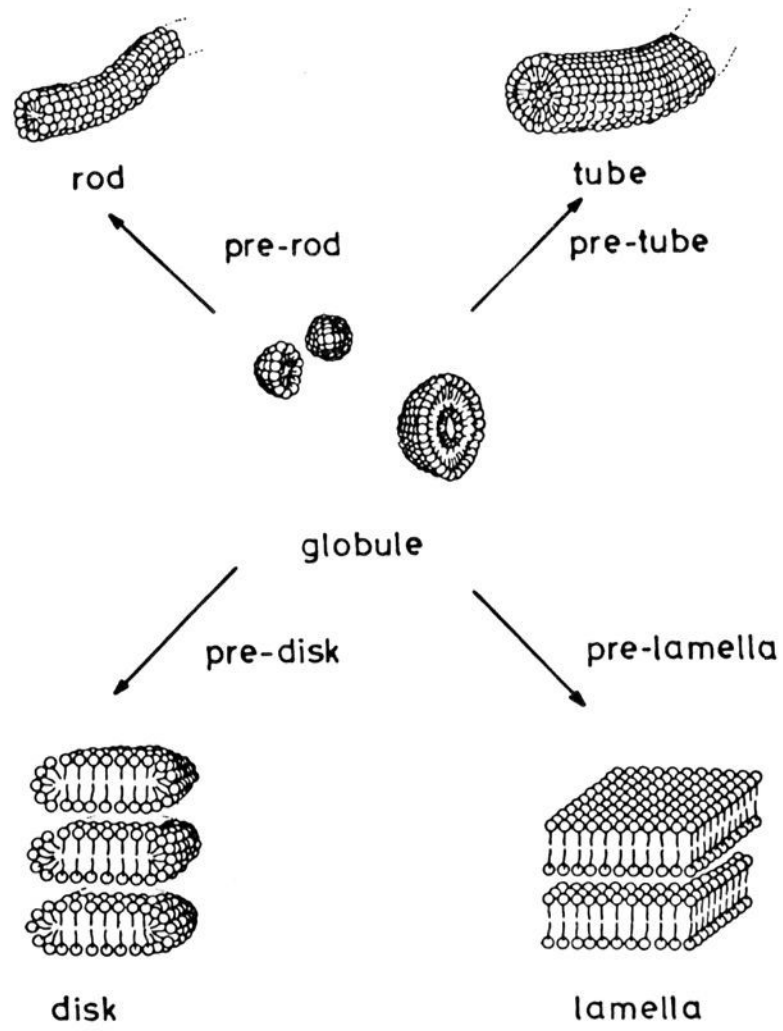

Figure 1. Schematic illustrations of the representative aqueous aggregates. The enhanced organization of globular aggregates leads to rod, tube, disk, and lamella. Incompletely developed structures are designated as pre-rod, pre-tube, etc.

Survey of Aggregate Morphologies. The aggregate morphology observed by electron microscopy is given in Table I for each amphiphile. The gel-to-liquid crystal phase transition, if detected by differential scanning calorimetry (DSC), would support the formation of the ordered structure. It must be emphasized that these measurements were performed for *dilute* aqueous solution of amphiphiles: 10 mM for electron microscopy and 30–40 mM for DSC. In the case of negative-staining electron microscopy, the sample solution was mixed with an aqueous solution of staining agents and was allowed to spread on a carbon-coated Cu grid as a thin film and dried. It is sometimes argued that the morphology of aqueous aggregates is not preserved at the stage of the electron microscopic observation under high vacuum. However, it has been proven for numerous biological samples that staining agents can fix the aggregate morphology. The morphology inferred for negatively stained samples is consistent with that of freeze-fracture replicas of the same aggregate, as shown later. The freeze-fracture sample is prepared by instantaneous freezing of aqueous samples and the original morphology should be preserved. We thus believe that electron micrographs of negatively stained samples reflect morphologies of the aqueous aggregate relatively faithfully.

The morphology given in Table I includes globules, vesicles, lamellae, rods, tubes, and disks. Their schematic illustrations are shown in Figure 1. A globule is a stable morphological entity and is different from fluid, globular micelles. The conventional fluid micelle such as the CTAB micelle does not give any definite structure by negative-staining electron microscopy. In spite of

(4) Kunitake, T.; Okahata, Y.; Tamaki, K.; Kumamaru, F.; Takayanagi, M., *Chem. Lett.* **1977**, 387–390.
(5) For reviews: (a) Kunitake, T., *J. Macromol. Sci.-Chem.* **1979**, *A13*, 587–602. (b) Fendler, J. H. *Acc. Chem. Res.* **1980**, *13*, 7–13.
(6) Kunitake, T.; Okahata, Y. *J. Am. Chem. Soc.* **1980**; *102*, 549–553.
(7) Okahata, Y.; Kunitake, T. *Ber. Bunsenges. Phys. Chem.* **1980**, *84*, 550–556.
(8) Okahata, Y.; Kunitake, T. *J. Am. Chem. Soc.* **1979**, *101*, 5231–5234.
(9) Gray, G. W. "Molecular Structure and the Properties of Liquid Crystals"; Academic Press: London, 1962.

the lack of fine structures, the phase transition is detected for some globules. Therefore, globules may be considered as collections of less developed (or fragmentary) lamellae.

The two-dimensional development of the bilayer assembly produces the typical bilayer membrane. The lamellar structure is stacks of the well-developed bilayer and the vesicles is made of closed bilayers. When the bilayer structure possesses high curvature and develops uni-dimensionally, rodlike and tubular structures will result. The rodlike structure is filled inside and the tubular structure has the inner aqueous hole. The discrimation between rods and tubes is made mainly by the diameter, but both aggregates look the same by electron microscopy. A combination of flat bilayers and portions of high curvature will produce disklike structures. The high-curvature portion constitutes the disk edge. The disklike structure may be isolated or it may exist in stacked forms. Thus, it is concluded that the fundamental structural unit of all the aggregate morphologies depicted in Figure 1 is the bilayer assembly.

Some of the aggregate morphologies are designated as no structure, pre-lamella, pre-rod, and pre-disk. An aggregate is designed as "no structure" when definite structures are not detected. The prefix "pre-" is used when the aggregate morphology is not sufficiently developed into the respective one.

It is interesting to compare these structures with those of micelles and lyotropic liquid crystals of conventional surfactants. Aqueous micelles of the conventional surfactant are spherical. When the aggregation number of surfactant molecules is increased due to the inherent amphiphilic property or due to the increase in the surfactant concentration, ellipsoidal micelles are formed. Further increases in the surfactant concentration may produce cylindrical micelles.[10] These micellar morphologies are similar to some of those (globules, rods, and disks) of Figure 1. However, micelles are in the dynamic equilibrium with free surfactant molecules and the micellar core is known to have the liquid-like fluidity,[2] unlike the highly ordered structure of the aggregate of Figure 1.

The lamellar structure and rodlike aggregates are formed in lyotropic liquid crystals of the conventional surfactant. The stability of these mesophases is, however, maintained by the intermicellar forces—i.e., the lattice forces—rather than forces from intramicellar close packing,[11] and will be lost when micelles are diluted. The ordered aggregate structures of Figure 1 are maintained even in dilute solution, and their stabilities come directly from molecular packing.

Structural Elements Which Determine the Aggregate Morphology. The extensive electron microscopic observation indicates that the aggregation behavior varies with the amphiphile structure according to fairly simple relations. It is convenient to consider that an amphiphile molecule is made of the following structural elements: (1) flexible tail, (2) rigid segment, (3) hydrophilic head group, (4) spacer group, and (5) additional interacting group. The influence of these structural elements on the aggregation behavior will be discussed below.

1. Flexible Tail. In a previous publication from these laboratories,[6] the bilayer formation was discussed for a series of ammonium amphiphiles which possessed the diphenylazomethine group as the rigid segment. Among these compounds (**1–9**), electron microscopy indicates that bilayer vesicles and lamellae are formed from **4–9**, but not from **1–3**. Amphiphile **3** has a C_4 tail and C_{10} spacer, and the combined length of the aliphatic chain (C_{14}) could be more than sufficient to form stable bilayers. The absence of the structure formation for **3** indicates that the length of the flexible tail, but not the length of the total methylene chain, is crucial for the bilayer formation. It is required that the flexible tail is not branched, since amphiphile **13** does not produce ordered aggregates. The branching in the alkyl tail may interfere with the molecular ordering, since the C_7 tail, if unbranched, should be long enough for the bilayer formation: **13** vs. **5**.

2. Rigid Segment. The rigid segment is probably the single, most important structural element in determining the aggregate morphology. Although our initial selection of the rigid segment was based on the aromatic structures which are found in typical liquid crystalline materials, other aromatic moieties listed under "other rigid segments" in Table I are similarly useful for controlling the aggregate morphology. The presence of at least two benzene rings appears necessary for the formation of stable bilayer assemblies,[12] since the structure formation is not detected for **10–12**. This supposition is reasonable, as conventional surfactants containing single benzene rings (alkylbenzenesulfonates, poly(oxyethylene)nonylphenol, etc.) form fluid micelles rather than bilayer membranes.

In the following is discussed the influence of the structure of rigid segments on the aggregate morphology. In order to separate the influence of the rigid segment from those of the other structural elements, a series of ammonium amphiphiles with the dodecyl tail and the tetramethylene spacer were selected and their aggregation behavior was examined closely as summarized in Table II.

These amphiphiles are classified into four groups according to the aggregate morphology. The first group contains the diphenylazomethine unit as the rigid segment. An electron micrograph (Figure 2a) of negatively stained aggregates of this amphiphile (**8**) shows the formation of multiwalled vesicles. The layer width is ca. 50 Å. A freeze-fracture-replica electron micrograph of Figure 2b more clearly shows the presence of spherical aggregates (vesicles) with a diameter of 500–1000 Å.

The second group of amphiphiles contains the biphenyl or azobenzene unit as the rigid segment. The formation of globular aggregates with a diameter of 200–300 Å is apparent for a negatively stained sample (Figure 2c) and for a freeze-fracture replica (Figure 2d). Almost identical morphologies were found for azobenzene-containing amphiphiles **40–43** and for azoxybenzene-containing amphiphile **49**.

The third group of amphiphiles gives very different morphologies. Their typical electron micrographs are given in Figures 2e–h. Figure 2e is obtained from a negatively stained sample of reduced diphenylazomethine amphiphile **54** and Figure 2f is a micrograph of the freeze–fracture replica of the same aggregate. The formation of the thread-like structure is seen beyond doubt. The individual molecule may exist in the aggregate in a rodlike arrangement or in a tubular arrangement; see Figure 1. The aggregate diameter in Figures 2e and 2f is approximately 100 Å. Since the extended molecular length of **54** is 36 Å, the rodlike structure is inconceivable. Figures 2g and 2h are again negative-staining and freeze-fracture replica micrographs, respectively, of the aggregate of **52**. The diameter in these cases is 60–70 Å, and the rodlike structure is more likely from the molecular length of 38 Å. Similar aggregate morphologies (rods or tubes) were found also for **14** (60–70 Å), **50** (70 Å), **51** (100 Å), **53** (50 Å), and **55** (100 Å). The aggregates diameters are given in parentheses.

The fourth group of amphiphiles, **62**, produces disklike aggregates as shown in Figure 2i. The disk is ca. 60 Å in thickness and 100–200 Å in diameter, and forms stacked arrays.

Other aggregation properties of these amphiphiles are included in Table II, together with those of CTAB. The cmc values are surprisingly insensitive to the difference in the chemical structure and are all close to 10^{-5} M. Amphiphile **62** give a little lower value due to an additional benzene ring in the rigid segment. A wide variation of the aggregate morphology is not reflected in the cmc value. The molecular structures of these amphiphiles are equivalent to that of CTAB plus rigid segments: the length of spacer group (C_4) plus flexible tail (C_{12}) is equal to that of the long alkyl chain (C_{16}) of CTAB. Therefore, insertion of the rigid segments lowers the cmc value by two orders of magnitude.

The aggregate weight varied over a range of 6×10^5 to 4×10^6. These values should be considered to be of the order-of-magnitude accuracy, and are of course much larger than that of

(10) Tanford, C. "The Hydrophobic Effect. Formation of Micelles and Biological Membranes"; Wiley-Interscience: New York, 1973; Chapter 9.
(11) Gray, G. W.; Winsor, P. A. *Adv. Chem. Ser.* **1976**, *No. 152*.
(12) The naphthalene and anthracene rings are effective rigid segments (M. Shimomura, unpublished results).

Table I. Amphiphiles and Their Aggregate Morphologies

A. Diphenylazomethine Group as Rigid Segment

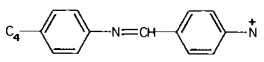

1, no structure

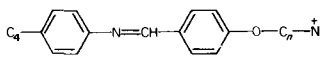

2 ($n = 4$), no structure
3 ($n = 10$), no structure

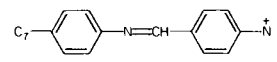

4, fingerprint-like

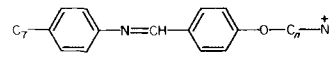

5 ($n = 4$), fingerprint-like
6 ($n = 10$), vesicle

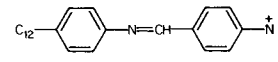

7, vesicle (multiwalled)

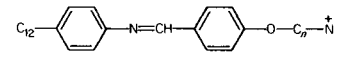

8 ($n = 4$), vesicle
9 ($n = 10$), vesicle and lamella

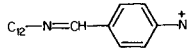

10, no structure

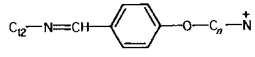

11 ($n = 4$), no structure
12 ($n = 10$), no structure

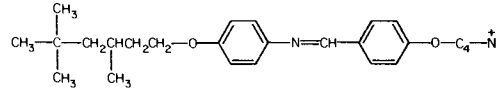

13, no structure

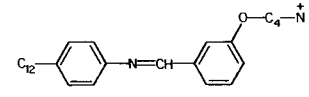

14, rod

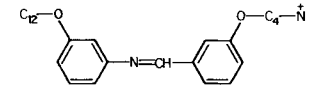

15, pre-rod and partial lamella

B. Biphenyl Group as Rigid Segment

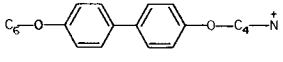

16, globule

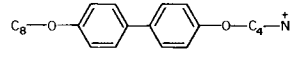

17, globule

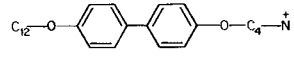

18, globule

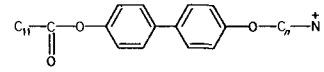

19 ($n = 4$), pre-disk
20 ($n = 10$), disk

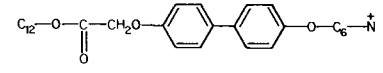

21, pre-disk

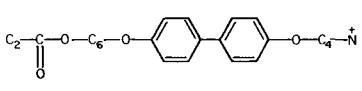

22, vesicle (multiwalled)

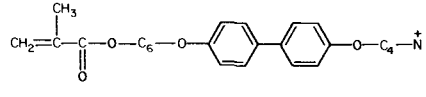

23, vesicle (multiwalled)

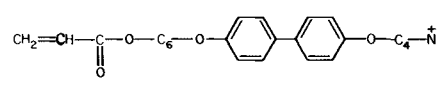

24, vesicle (mostly single walled)

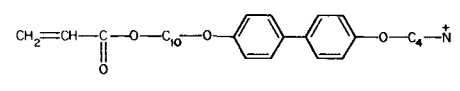

25, large vesicle

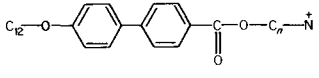

26 ($n = 3$), globule
27 ($n = 10$), disk

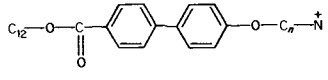

28 ($n = 4$), globule
29 ($n = 10$), stacked disk

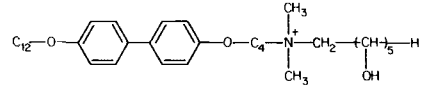

30, globule

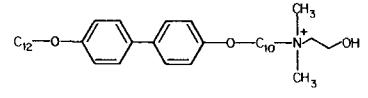

31, pre-rod

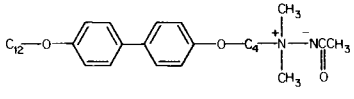

32, pre-vesicle

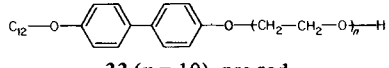

33 ($n = 10$), pre-rod
34 ($n = 15$), rod
35 ($n = 20$), stacked rod

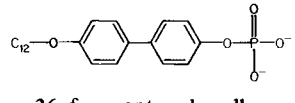

36, fragmentary lamella

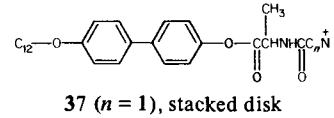

37 ($n = 1$), stacked disk
38 ($n = 5$), stacked disk

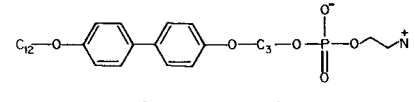

39, stacked disk

C. Azobenzene or Azoxybenzene Group as Rigid Segment

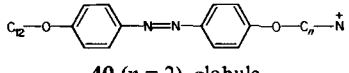

40 ($n = 2$), globule
41 ($n = 4$), globule
42 ($n = 10$), globule

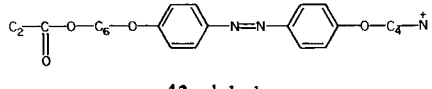

43, globule

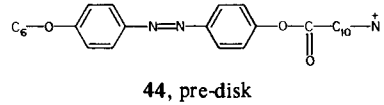

44, pre-disk

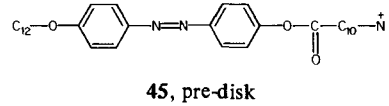

45, pre-disk

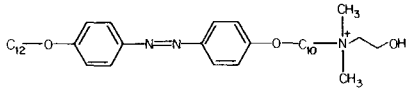

46, pre-rod

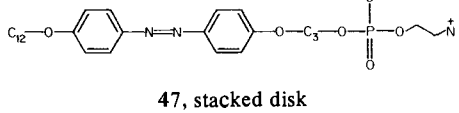

47, stacked disk

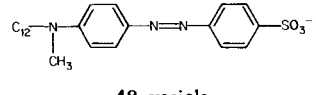

48, vesicle

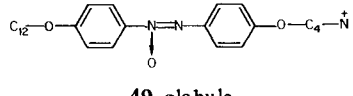

49, globule

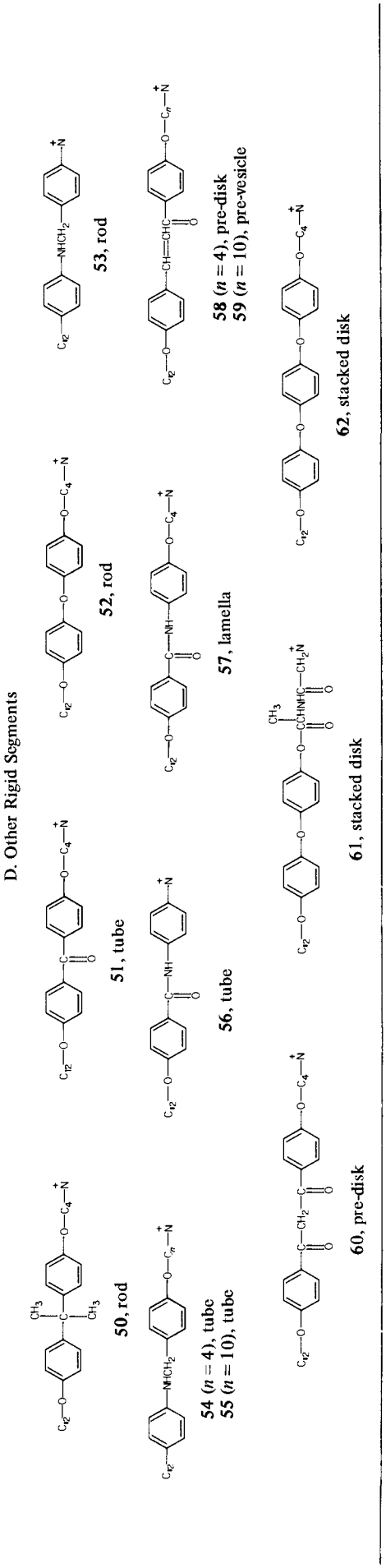

the CTAB micelle. Amphiphile **8** gives the largest value. The amphiphiles belonging to the second and third groups show analogous aggregate weights of (6–8) × 10^5, and **62** shows a larger value of 1.2 × 10^6.

The restricted motion of amphiphilic molecules in the aggregate can be assessed from NMR line broadening and by differential scanning calorimetry. Figure 3 contains NMR spectra of an aqueous (D_2O) solution of the representative ammonium amphiphiles. The line widths of the methylene and *N*-methyl protons are given in Table II. The line broadening was large for amphiphiles **8** and **62**. The other amphiphiles of Table II give a little smaller broadening. The different extents of the observed line broadening are consistent with the phase transition behavior. Figure 4 shows typical DSC thermograms of the aqueous aggregate. The reported thermogram for **8** is included for comparison. These endothermic peaks (in the heating cycle) are attributed to the gel-to-liquid crystal phase transition of the bilayer. The transition temperature and the enthalpy change are summarized in Table II. Distinct peaks are observable for aggregates of **8**, **18**, **52**, and **62**. The enthalpy changes found (0.4-3.8 kcal/mol) are decidedly smaller than those found for the bilayer of dialkyl amphiphiles. The ΔH value for most dialkylammonium bilayers is about 10 kcal/mol.[13] The phase transition was not detected ($\Delta H < 0.1$ kcal/mol) for the amphiphiles with bent rigid segments, except in the case of **52**. Since the extent of NMR line broadening is smaller than those of the other classes of amphiphile, these amphiphiles may be packed less tightly in the aggregate.

These aggregation behaviors, in particular morphologies, can be explained as arising from different characteristics of the rigid segment. In the first, when the rigid segment is biphenyl or azobenzene, globular aggregates (probably collections of small bilayer assemblies) are formed. The diphenylazomethine group is structurally very similar to the azobenzene group, but their behavior as the rigid segment is quite different, and well-developed bilayer membranes are formed from the amphiphile with the diphenylazomethine group. This difference appears to come from the dipolar nature of the rigid segment. It is generally accepted in the liquid crystal research that the molecular dipole plays an important role for alignment of molecules. In the same way, the dipolar interaction among the diphenylazomethine groups would promote formation of the well-organized bilayer. The symmetrical rigid segment (biphenyl and azobenzene) can produce the bilayer assembly, but the extensive organization appears difficult.

A structural feature common to the third group of amphiphiles is that they contain the bent rigid segment. Figure 5 shows the projection of the CPK molecular models. The molecules are bent at the rigid segment due to the single-atom connection of the two benzene rings (**50**, **51**, and **52**), due to rotation of the single bond (**54** and its analogues), or due to the meta substitution (**14**). The CPK molecular model of linear **8** is shown for comparison. The rigid segment is straight in this case. The contrasting behavior of the straight and bent ammonium amphiphiles is interesting. It is suggested that the straight molecules such as **8** tend to assemble in the neat, two-dimensional arrangement (membrane), but that the bent molecules give rise to curvatures which result in the radial molecular arrangement (rodlike and tubular structures). The double-meta substitution at the rigid segment as in **15** produces less organized aggregates. Too much bending is not advantageous for molecular ordering.

The disk structure contains two kinds of molecular arrangement. One is the two-dimensional arrangement (flat portion) as in the typical bilayer membrane and the other is highly curved arrangements (side of the disk) as in the rodlike structure. Amphiphile **62** can assume two conformations as shown in Figure 6. These two conformations may be used advantageously for producing the two kinds of molecular packing required for the disk. The ratio of the two conformers apparently depends on the extent of molecular dispersion, since lamellae are abundantly observed in some cases. The latter structure should contain only

(13) Okahata, Y.; Ando, R.; Kunitake, T. *Ber. Bunsenges. Phys. Chem.*, in press.

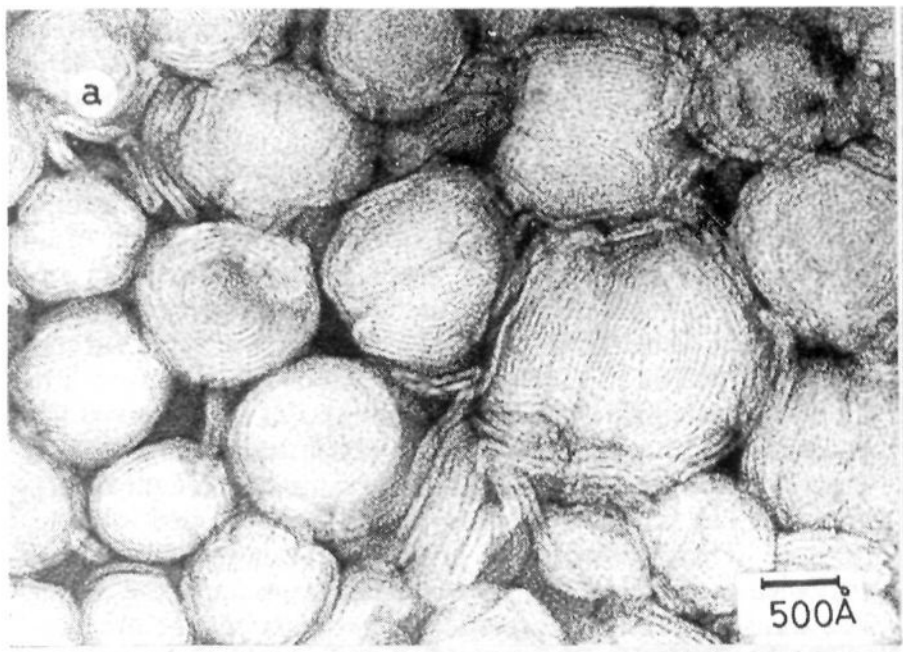
a
500Å

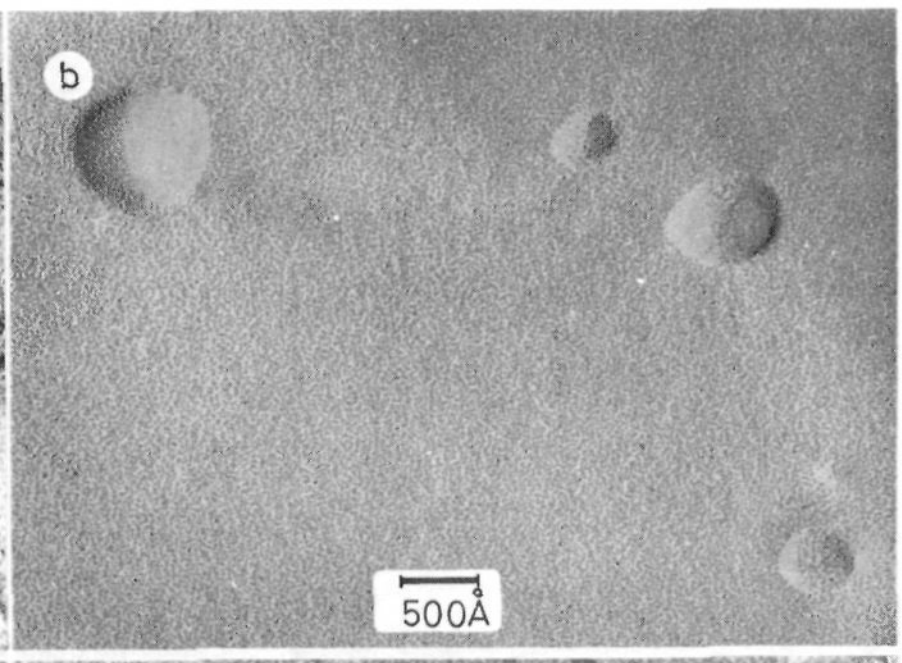
b
500Å

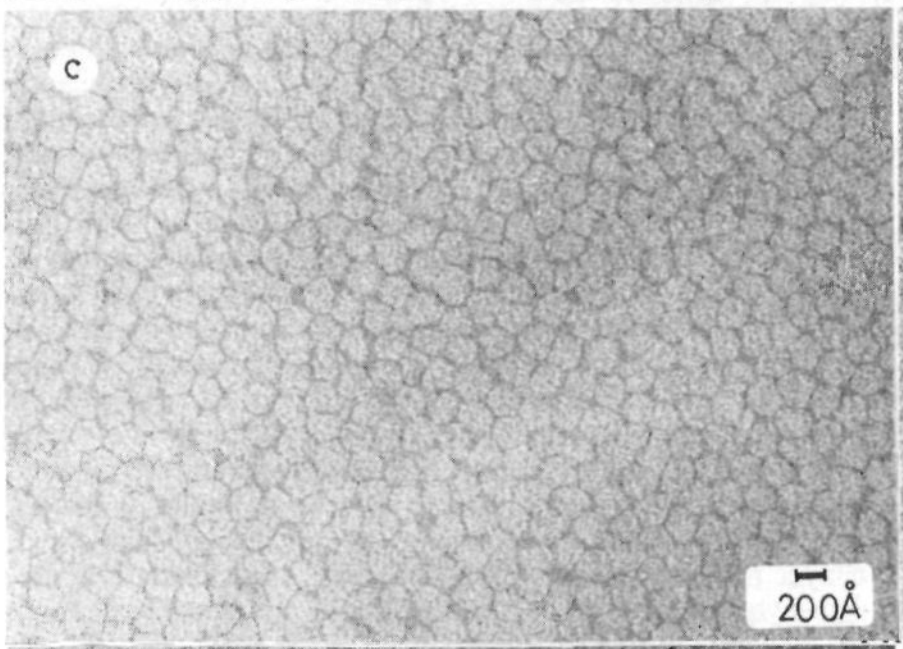
c
200Å

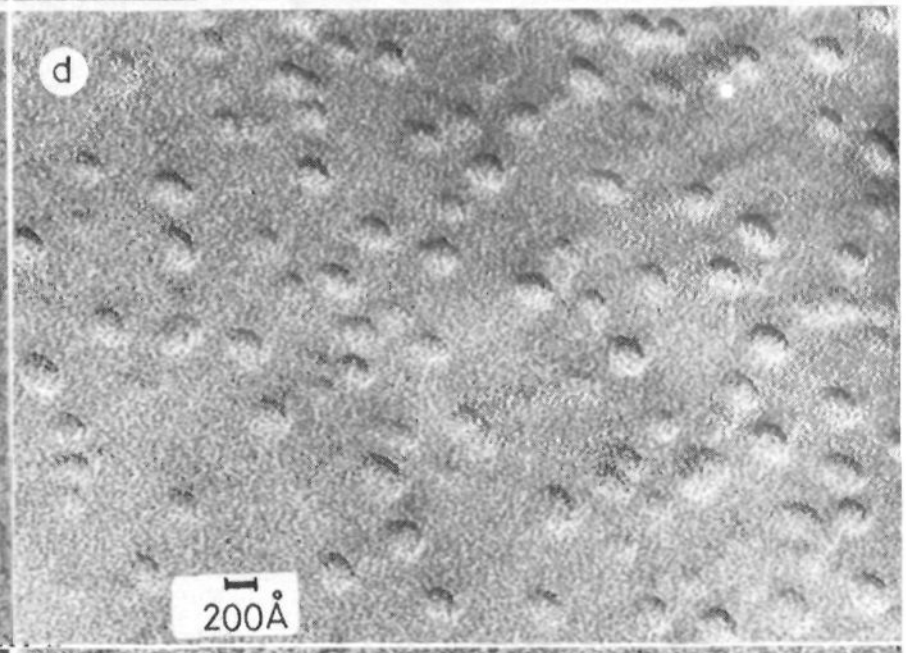
d
200Å

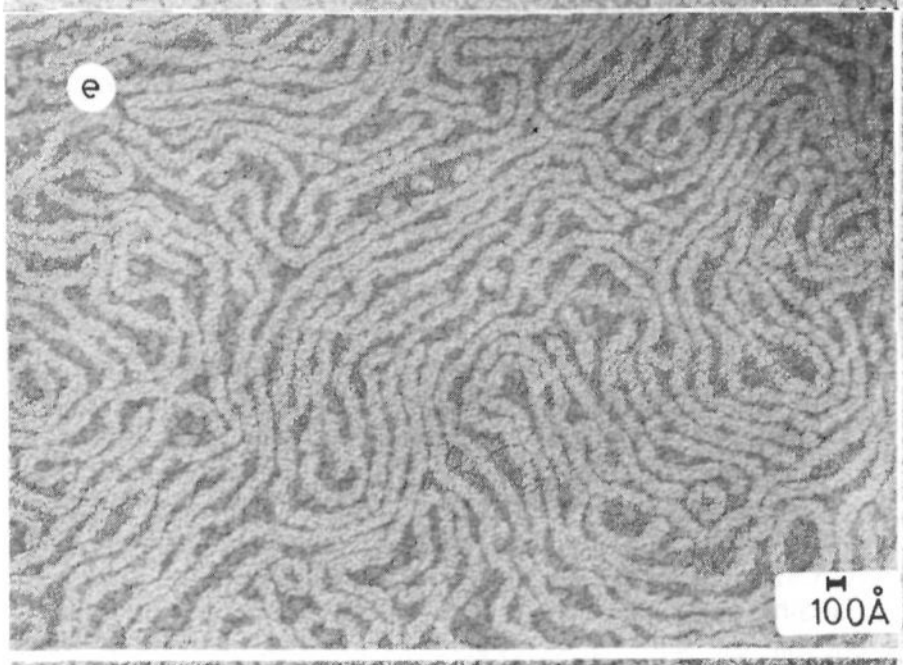
e
100Å

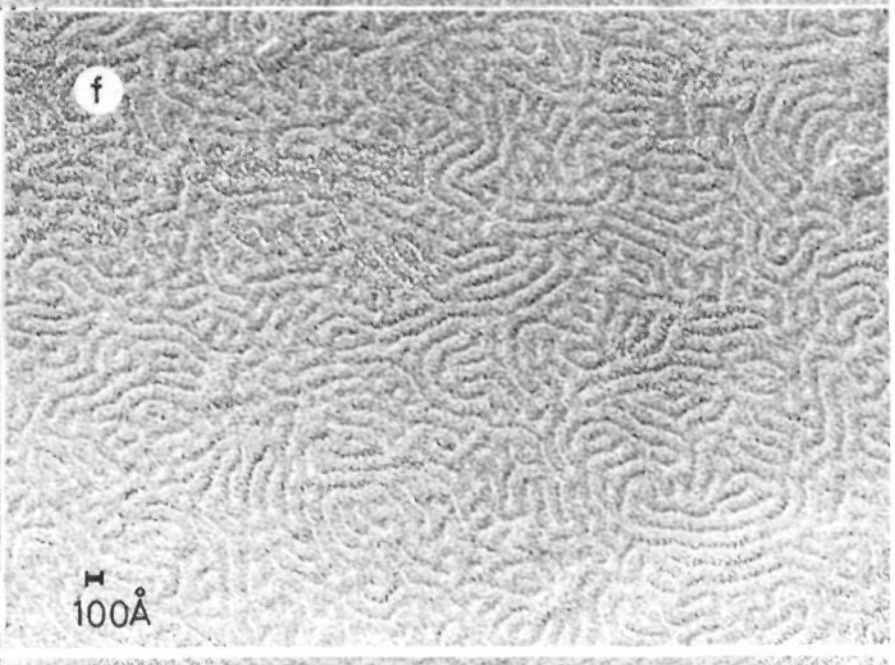
f
100Å

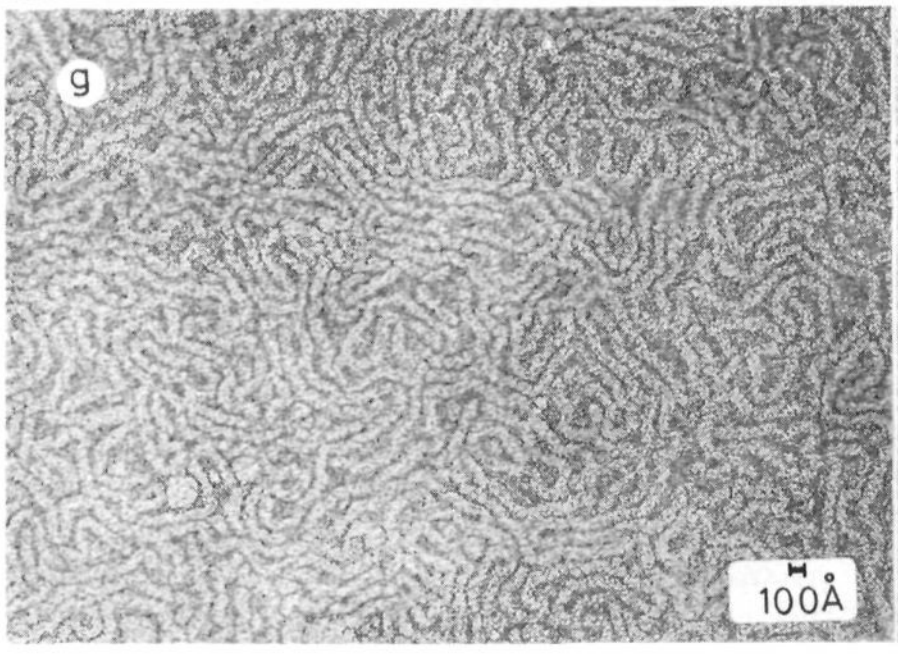
g
100Å

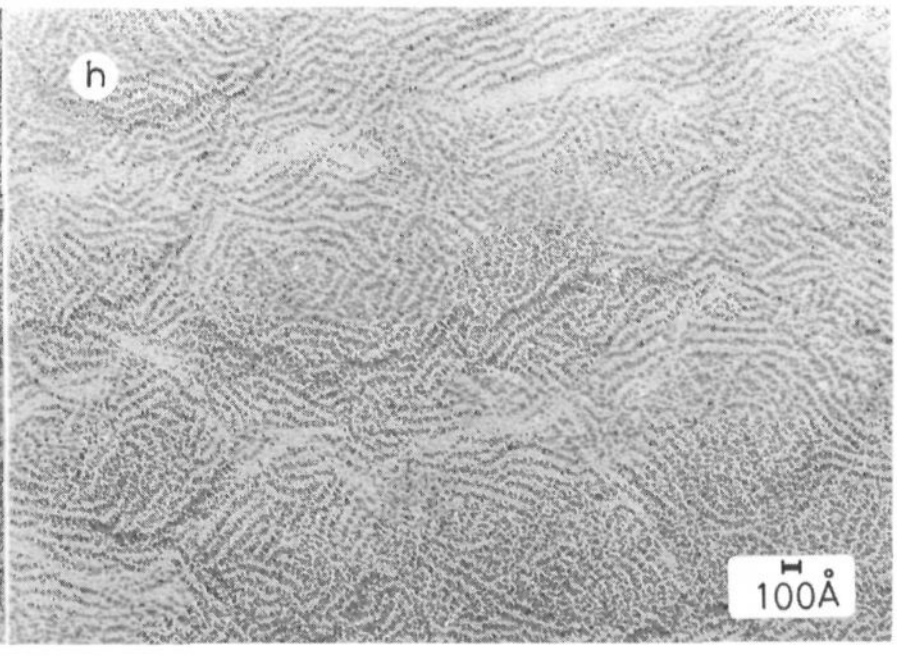
h
100Å

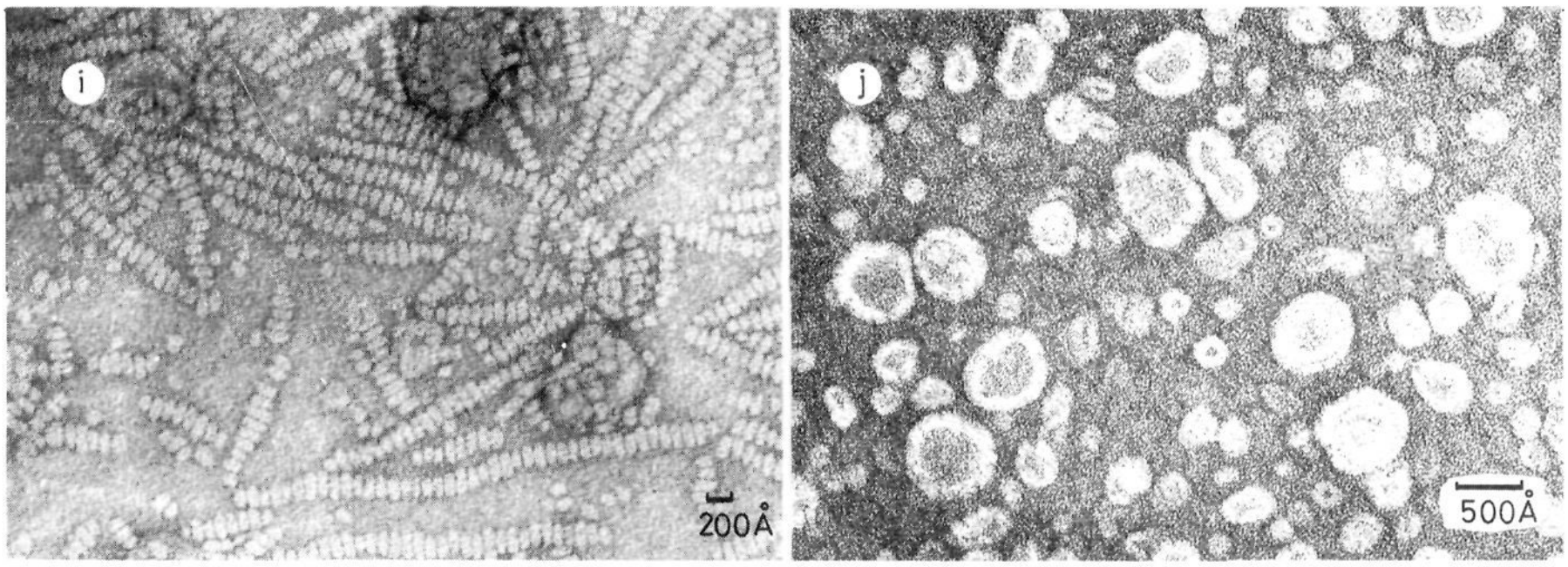

Figure 2. Electron micrographs of the single-component aggregates, magnification ×150 000: (a) amphiphile **8**, negative staining; (b) amphiphile **8**, freeze fracture replica; (c) amphiphile **18**, negative staining; (d) amphiphile **18**, freeze fracture replica; (e) amphiphile **54**, negative staining; (f) amphiphile **54**, freeze fracture replica; (g) amphiphile **52**, negative staining; (h) amphiphile **52**, freeze fracture replica; (i) amphiphile **62**, negative staining; (j) amphiphile **24**, negative staining.

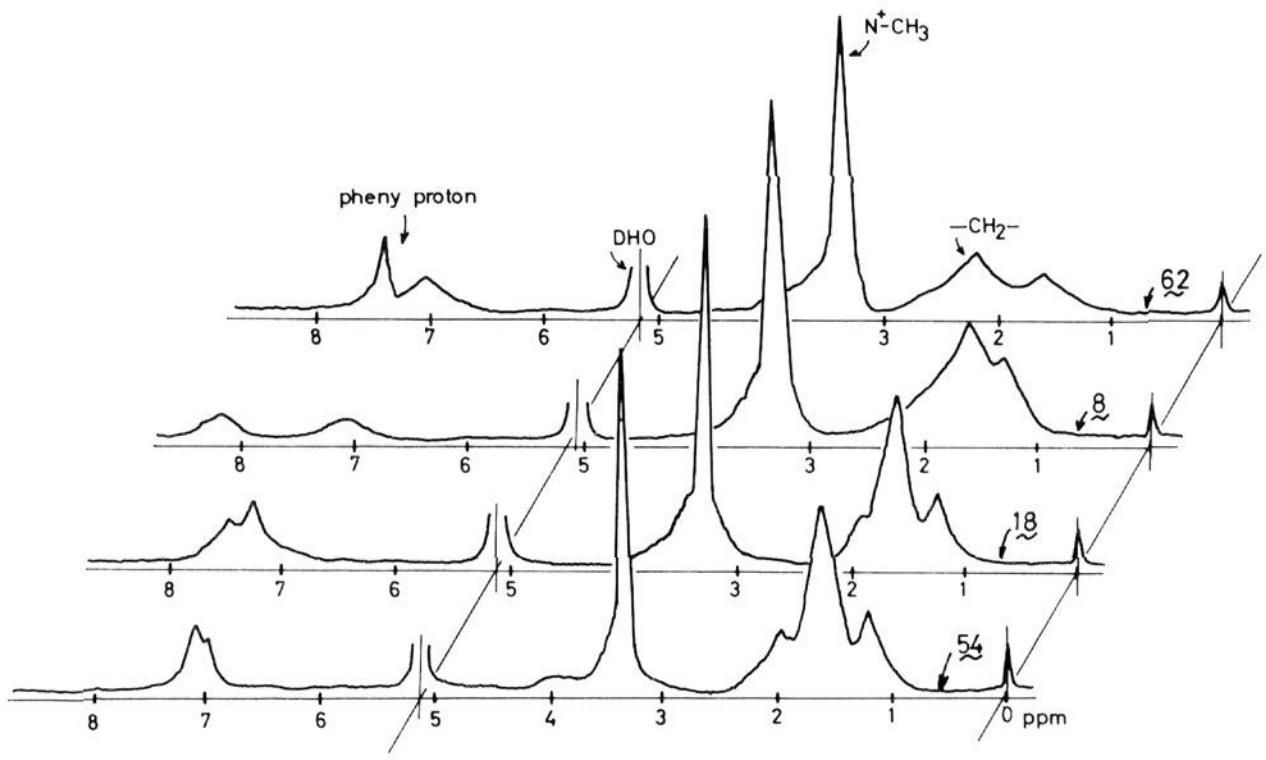

Figure 3. ^{1}H NMR spectra of amphiphiles in D_2O: concentration 0.5 wt % (ca. 10 mM), 2000–4000 scan, internal reference DSS, instrument Bruker WH-60.

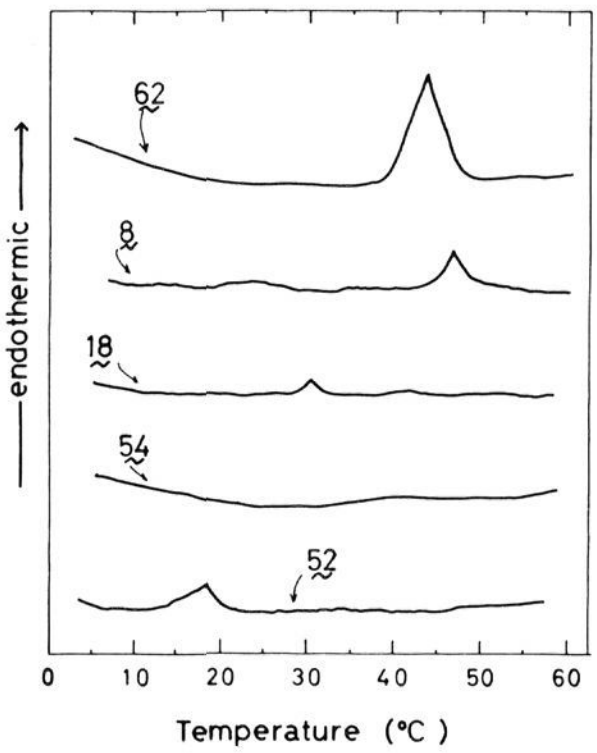

Figure 4. Differential scanning calorimetry of aqueous aggregates: concentration 1–2 wt %, heating rate 2 °C/min.

the extended conformer of **62**. A question which remains unanswered is why disks stack. There appears to be no reason for positively charged disks to form stacked arrays. It is interesting in this respect that very similar stacked disks are found for a protein–lecithin complex, in which the lecithin bilayer produces the flat portion and apolipoproteins occupy the side of the disk.[14]

The disklike aggregate was also found for **20**, **27**,[15] **29**,[15] **37**,[16] **38**,[17] **39**,[18] **47**,[18] and **61**.[17] These amphiphiles contain additional interacting groups or other hydrophilic head groups, and their morphologies cannot be discussed only in terms of the rigid segment (see below).

Amphiphiles **58**[19] and **60**[19] have the same tail (C_{12}) and spacer (C_4) with presumably less rigid segments. They form pre-disk aggregates. The molecular assembling is apparently not complete with these rigid segments.

(14) Wlodawer, A.; Segrest, J. P; Chung, B. H.; Chiovetti, R., Jr.; Weinstein, J. H. *FEBS Lett.* **1979**, *104*(2), 231–235.
(15) Horimoto, A., unpublished preparation in these laboratories.
(16) Kunitake, T.; Nakashima, N.; Morimitsu, K. *Chem. Lett.* **1980**, 1347–1850.
(17) Morimitsu, K., unpublished preparation in these laboratories.
(18) Okahata, Y.; Ihara, H.; Shimomura, M.; Tawaki, S.; Kunitake, T. *Chem. Lett.* **1980**, 1169–1172.
(19) Yasunami, S., unpublished preparation in these laboratories.

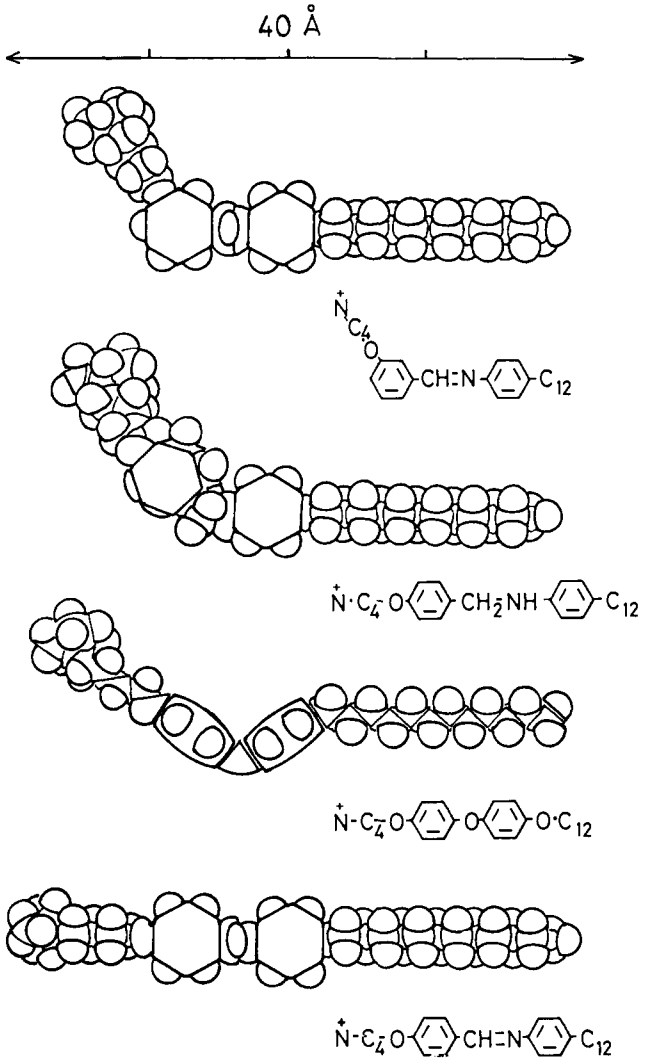

Figure 5. Projections of the CPK molecular model of bent and linear ammonium amphiphiles.

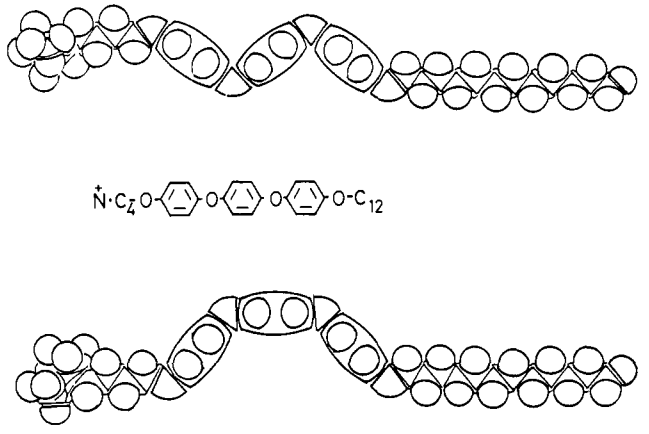

Figure 6. Extended and bent conformations of **62**.

3. Hydrophilic Head Group. The aggregate morphology is affected by the kind of hydrophilic head group. This problem has been partly discussed in a recent publication from these laboratories for amphiphiles with the biphenyl rigid segment.[7] The single-chain ammonium amphiphile with biphenyl rigid segment **18** produces globular aggregates. The modification of the trimethylammonium group by attachment of a sugar moiety (**30**) does not change the morphology, but the introduction of the hydroxyethyl group as in **31**[20] and the conversion to the zwitterionic group (**32**) appear more effective. The introduction of the zwitterionic phosphocholine moiety as in **39** produces disklike aggregates.[18]

Clear bilayer formation is observed when the trimethylammonium head group is replaced by anionic (phosphate) or nonionic (poly(oxyethylene)) groups (**33–36**). Apparently, the latter head groups induce more definite membrane surfaces. The length of the poly(oxyethylene) chain is influential, because the morphology changes from pre-rods to rods to stacked rods with increasing oxyethylene chain lengths.

The morphological influence of the head group is found also for other rigid segments. Ammonium amphiphiles with azobenzene rigid segment **40–42** produce globular aggregates devoid of fine structures. Modification of the trimethylammonium group by the hydroxyethyl group (**46**)[20] gives pre-rod aggregates. Furthermore, stacked disks are formed when the phosphocholine residue is used as the head group (**47**),[18] and bilayer vesicles are found with the sulfonate head group **48**.[21] The enhanced dipolar property of the rigid segment in **48** should be advantageous for the bilayer formation. It appears that the trimethylammonium head group is not particularly effective for aligning amphiphilic molecules.

4. Spacer Group. The spacer group—the flexible chain which connects the hydrophilic head group and the rigid segment—generally improves the molecular alignment. However, its effectiveness depends on the extent of molecular assemblage without the spacer group. Thus, in the case of a group of amphiphiles which contain the diphenylazomethine rigid segment and the C_{12} tail, multiwalled bilayer vesicles are observed without the spacer group, **7**. Introduction of the C_4 and C_{10} spacers (**8** and **9**, respectively) does not cause appreciable morphology changes, but some lamellar structures are detected for **9**. The spacer effect is more apparent when the flexible tail is C_7. In this case, the bilayer assembly is less developed (fingerprint-like) for those amphiphiles that possess no spacer (**4**) or a C_4 spacer (**5**), but vesicles are found for **6** that possess a C_{10} spacer.

The spacer effect is also apparent for amphiphiles with the biphenyl rigid segment. The globular structure of **26** (C_3 spacer) is converted to disk-shaped aggregates in **27** (C_{10} spacer).[15] A similar effect (pre-disk → disk) is observed between **19** (C_4 spacer) and **20** (C_{10} spacer). The rod-like structure of **53** (no spacer) is convered to the tubular structures in **54** (C_4 spacer) and **55** (C_{10} spacer), and the tubular structure of **56** (no spacer) changes to the lamellar structure of **57** (C_4 spacer).

In the case of the ammonium amphiphile with the azobenzene rigid segment, analogous, globular aggregates are found for **40** (C_2 spacer), **41** (C_4 spacer), and **42** (C_{10} spacer). The spacer effect is not apparent in morphology, but the increasing bilayer stability is revealed by elevating T_c values: 16, 25, and 46 °C for **40**, **41** and **42**, respectively.[20] In the case of a pair of chiral amphiphiles **37** and **38**, well-defined stacked disks are found without the influence of the spacer.

It is suggested from the above-mentioned examples that the spacer effect is most pronounced when the morphological influence of the rigid segment is not too strong. For example, the diphenylazomethine segment can promote the molecular orientation efficiently by itself and the spacer effect is not visible. The molecular alignment effect of the azobenzene unit is small, at least in terms of morphology, and even the C_{10} spacer cannot produce the well-developed bilayer structure. The biphenyl group seemingly possesses the intermediate orientational influence, and, therefore, the aggregate morphology can be controlled by changing the spacer length. The presence of a strongly interacting group in the spacer position (**37** and **38**) diminishes the spacer effect.

5. Additional Interacting Group. The data of Table II suggest that the dipolar nature of the rigid segment helps improve the intermolecular alignment. The validity of this suggestion is readily confirmed by introducing additional interacting groups into the single-chain amphiphile. Most dramatic examples are found for

(20) Shimomura, M., unpublished preparation in these laboratories.

(21) Kunitake, T.; Nakashima, N.; Shimomura, M.; Okahata, Y.; Kano, K.; Ogawa, T. *J. Am. Chem. Soc.* **1980**, *102*, 6642–6644.

Table II. Influence of Rigid Segments on the Aggregation Behavior of Ammonium Amphiphiles[a]

compd	rigid segment	$10^5 \times$ cmc, M	aggregate wt	line width of NMR spectra in D_2O, Hz		phase transition T_c, °C (ΔH, kcal/mol)	aggregate morphology
				$-CH_2-$	N^+-CH_3		
CTAB	none	80	4×10^4	5	3	no peak	no structure
8	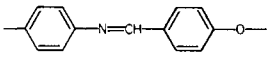	1.0	4×10^6	30	11	47 (1.4)	multiwalled vesicle
18	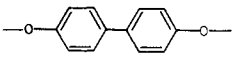	0.8	8×10^5	27	6	30 (0.4)	globule
41	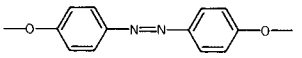		2.4×10^5			25 (2.9)	globule
50	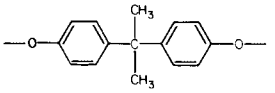	1.0	7×10^5	25	4	no peak	rod
51	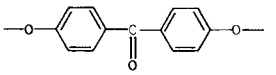	1.2	6×10^5	25	7	no peak	tube
52	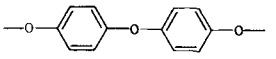	1.0	7×10^5	24	6	18 (1.6)	rod
53	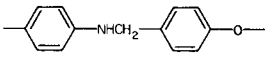	1.2	7×10^5	23	6	no peak	tube
14	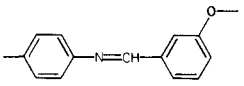	1.0	6×10^5	25	7	no peak	rod
62	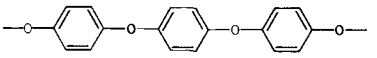	0.6	1.2×10^6	30	10	44 (3.8)	disk

[a] General structure of the amphiphiles: $C_{12}H_{25}$-(rigid segment)-$(CH_2)_4$-$N^+(CH_3)_3Br^-$.

biphenyl-containing ammonium amphiphiles. When the acrylate group is incorporated into the flexible tail, the globular aggregate of **18** (Figures 2a and 2b) is transformed into closed vesicles of **24** (Figure 2j). The vesicles possess diameters of 300–700 Å and most of them are single walled. This highly contrasting aggregation behavior is produced by the introduction of the polar ester group at the tail end. Similarly improved assemblage (vesicles) is observed for **22**, **23**, and **25**. When the ester group is located close to the biphenyl rigid segment, the disklike structure prevails in place of vesicles. Amphiphiles **19** and **20** give pre-disks and disks, respectively, and amphiphile **21** produces pre-disks. Similar results were obtained for amphiphiles **26–29** which contain the ester group directly bonded to the biphenyl rigid segment.

The effect of the ester is less pronounced with the azobenzene rigid segment. This is most clearly illustrated by a comparison of **22** and **43**. Amphiphile **22** produces multiwalled vesicles, but **43** gives globular aggregates in spite of the propionate ester present at the tail end. The ester group in **44**[22] and **45**[22] promotes the structure formation, since the corresponding amphiphile without the ester group (**42**) forms globular aggregates.

The effectiveness of the ester group to promote formation of the bilayer assemblage was amply demonstrated for the dialkyl amphiphile.[24]

A second example of the additional interacting group is found in the aggregation behavior of **37**,[16] **38**,[17] and **61**.[17] These amphiphiles possess the alanyl residue in the spacer position, and produce stacked disks. In the absence of the alanyl residue, globular aggregates (**18**) or rodlike aggregates (**52**) are obtained. The amide and ester groups are introduced along with the alanyl residue, and these interacting groups may be able to modify the aggregate morphology, though the influence of the chiral carbon is also conceivable.

The Morphology of Two-Component Systems. In the preceding discussion, it is shown that the bent rigid segment gives enhanced surface curvature to the aggregate. Then it may be asked if the surface curvature of the aggregate can be controlled by appropriate combinations of different classes of amphiphile. Figure 7 shows a series of electron micrographs which were obtained for mixtures of **8** and **52**. These amphiphiles possess the identical structural elements except for the rigid segment. As mentioned above, **8** produces well-developed bilayer vesicles (Figures 2a and 2b) and **52** produces tubular aggregates (Figures 2g and 2h). Thread-like structures similar to Figure 2g (diameter 70–80 Å) are found for a 1:1 mixture of **8** and **52** (Figure 7a). An electron micrograph of a 7:3 mixture (Figure 7b) shows the presence of flat vesicles (or disks) and thread-like structures. A 9:1 mixture (Figure 7c) produces stacked disks (or stacked patches of bilayers) with layer thickness of 40–50 Å. It is conceived that the flat portion of the disk is composed of **8**, and that **52** is concentrated in the side of the disk where large curvature is required.

Another interesting morphological change obtained by the mixing of amphiphiles is illustrated by Figure 7d. This is an electron micrograph of a 9:1 mixture of **8** and **18**. Amphiphile **8** forms multiwalled vesicles (Figure 1a) and **18** gives globular aggregates, but their 9:1 mixture produces single-walled vesicles. Similar, single-walled vesicles are found for a 9:1 mixture of **8** and **41** (rigid segment, azobenzene).

The morphological change due to addition of second components has been found in several other instances. Addition of equimolar amounts of **9** or nonionic dialkyl amphiphile $2C_{12}$-gl-15G transformed the multiwalled vesicles of **7** into single-walled vesicles.[6] Cholesterol which is abundantly present in the animal

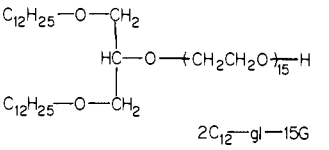

plasma membrane was shown to be quite compatible with the synthetic bilayer system, with the resulting morphological change. For example, addition of a third molar of cholesterol transformed globular aggregates of **30** and rodlike aggregates of **34** into sin-

(22) Ihara, H., unpublished preparations in these laboratories.
(23) Hashimoto, M., unpublished preparation in these laboratories.
(24) Kunitake, T.; Nakashima, N.; Hayashida, S.; Yonemori, K. *Chem. Lett.* **1979**, 1413–1416.

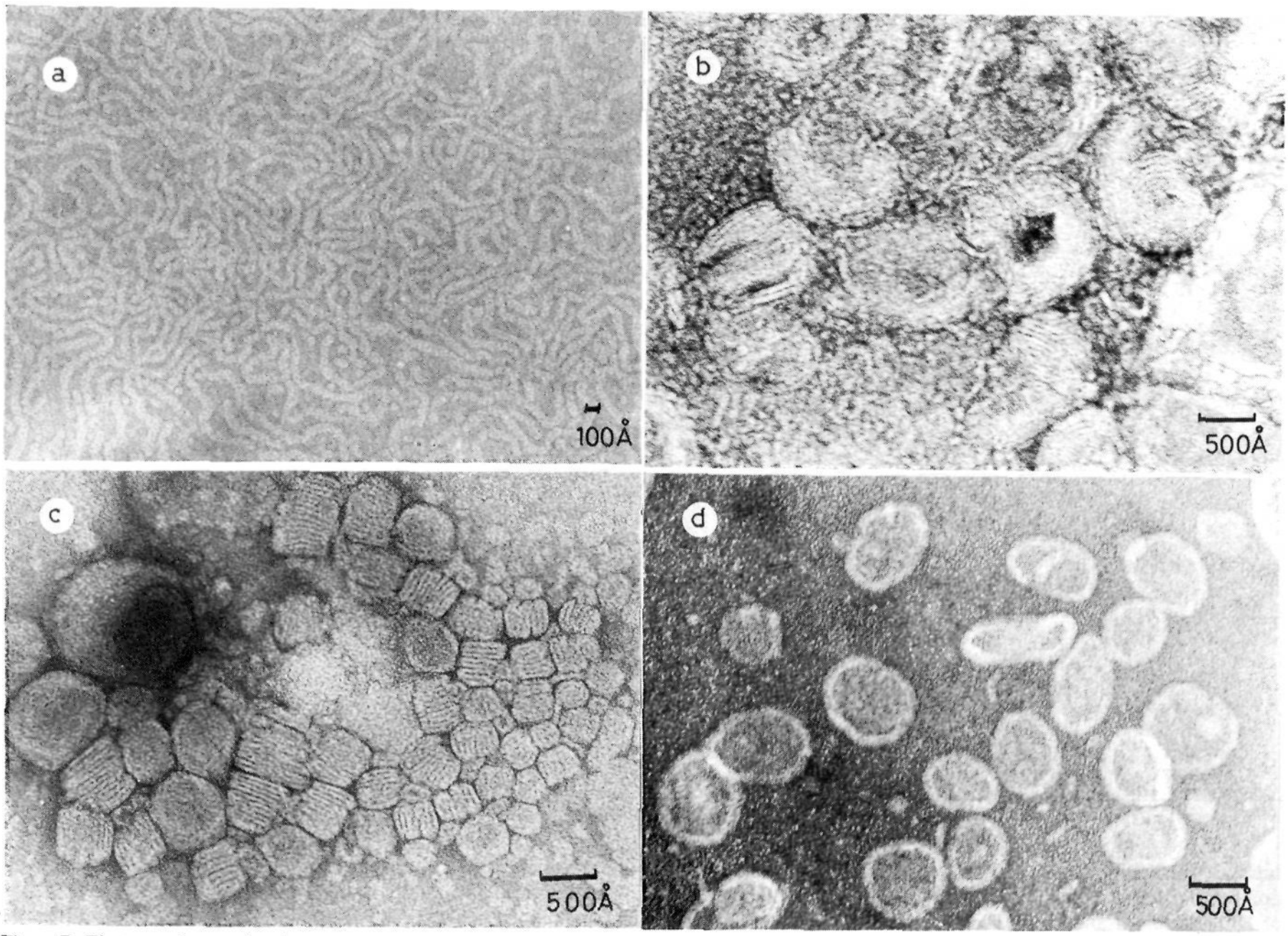

Figure 7. Electron micrographs of some two-component aggregates, magnification ×150 000, negative staining with uranyl acetate: (a) 5:5 molar mixture of **8** and **52**; (b) 7:3 molar mixture of **8** and **52**; (c) 9:1 molar mixture of **8** and **52**; (d) 9:1 molar mixture of **8** and **18**.

gle-walled and flattened vesicles, respectively,[7] and lamellar monolayers of a two-headed ammonium amphiphile were converted to single-walled vesicles by cholesterol addition.[8]

It is clear from these examples that mixing of appropriate membrane components is a powerful technique in controlling the aggregate morphology.

Dynamic Control of the Aggregate Morphology. The aggregate morphology is determined by the chemical structure of the component amphiphile. This is considered as a *static* control of the morphology. The dynamic morphology control is rendered possible as an extension of the present research. The azobenzene chromophore undergoes the cis–trans isomerization. The *trans*-azobenzene unit assumes the extended geometry and the globular aggregates are formed from simple azobenzene-containing amphiphiles **40–42**. On the other hand, the *cis*-azobenzene unit possesses the bent geometry and should act as a bent rigid segment similar to those of **50–52**. Upon partial trans-to-cis isomerization, the globular aggregates of **40–42** are transformed into the cylindrical aggregates.[21] The light-induced morphology change should be possible for other amphiphiles which contain photoreactive moieties. We have found that the bilayer structure is formed from ammonium amphiphiles which contain the anthracene, stilbene, and stilbazole units as the rigid segment.[23] The photochemical investigation of these aggregates is in progress.

Aggregate Morphology and Fluorescence Intensity. The change in the aggregate morphology leads to the variation of other physicochemical characteristics. For example, the packing of the rigid segment in aqueous aggregates would be varied with the aggregate morphology. This is indicated by the fluorescence behavior of the aggregate of the biphenyl-containing ammonium amphiphiles. Figure 8 describes some of the temperature dependence of the fluorescence intensity. The temperature dependence is represented by two patterns: one is the increase in the

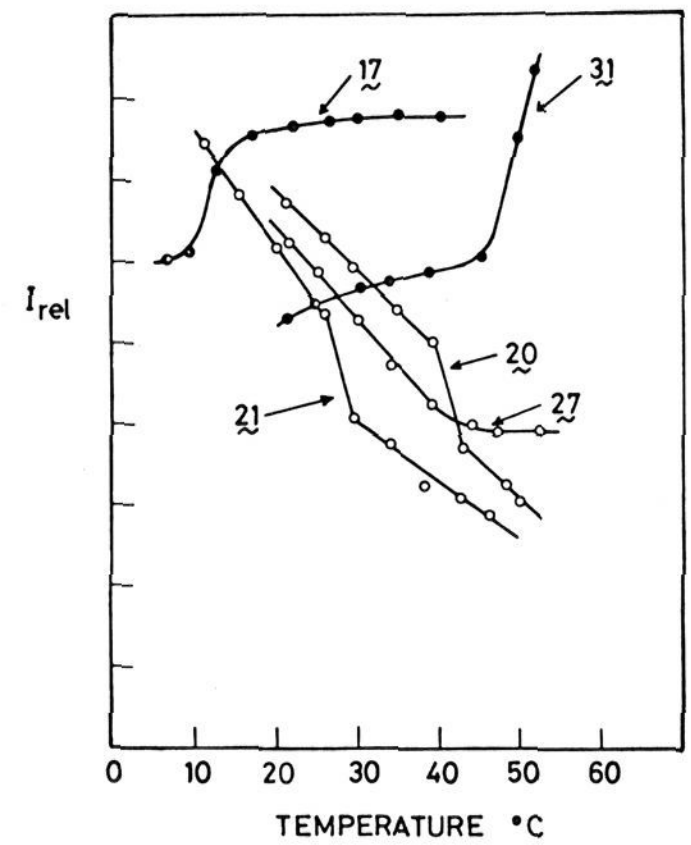

Figure 8. Temperature dependence of fluorescence intensity of some aqueous amphiphiles (see Table III).

fluorescence intensity with temperature (up) and the other is the decrease with temperature (down). The inflection region is observed for both cases. Table III summarizes the fluorescence behavior for the aggregate of nine amphiphiles. These amphiphiles contain the biphenyl rigid segment and the ammonium head group in common, and their morphological variation is induced by the

Table III. Aggregate Morphology and Fluorescence Characteristics[a]

amphiphile	aggregate morphology	temp dependence of fluorescence inten	inflection region, °C	T_c, °C
17	globular	up	16	n.d.[b]
26	globular	up	34	(20-30)[c]
31	pre-rod	up	46	44.5
19	pre-disk	down	12-16	n.d.
21	pre-disk	down	25-30	25
20	disk	down	39-44	45
27	disk	down	42	42
37	disk	down	37.5	35
38	disk	down	n.d.	n.d.

[a] Amphiphiles ca. 1×10^{-4} M, excitation wavelength (E_x) 300 nm, emission wavelength (E_m) 350 nm. However, E_x = 320 nm and E_m = 430 nm for **26**, and E_x = 320 nm and E_m = 390 nm for **27**. [b] n.d., not detected. [c] Not very clear.

change in the spacer length amd the additional interacting group. Apparently, the mode of the temperature dependence (up and down) reflects the aggregate morphology. The up mode is observed for globules and closely related pre-rod aggregates, and the down mode is observed for disk and pre-disk aggregates. These results may be explained by assuming different orientations of the rigid segment in the two types of aggregate. The change of the molecular orientation is also reflected in the presence of the inflection region at or near T_c. The degree of polarization decreases from 0.18 to 0.08 with an increase in temperature across T_c in the case of **31** (pre-rod) but does not vary at T_c in the case of **27** (disk) (P = 0.22). We suggest that the molecular packing in the globular and pre-rod aggregates is looser than that in the disk-shaped aggregate.

Concluding Remarks. We attempted in this article to show what structural elements determine the aggregate morphology of single-chain amphiphiles. The most essential structural elements are flexible tail, rigid segment, and hydrophilic head group. The stable self-assembly will not be formed without either one of these elements. The other two elements, spacer group and additional interacting group, also affect the self-assembling behavior. The combination of these elements leads to a variety of the aggregate morphology observed for 62 single-chain amphiphiles.

An extensive morphological variation is similarly observed for the monolayer membrane of two-headed ammonium amphiphiles.[8] The structural factor which governs the aggregate morphology is different between the monolayer and bilayer assemblies. This problem will be discussed in a later publication.

The morphological variation has been reported for liposomes of the phospholipid. Bangham and Horne described in their classical paper[25] a variety of morphologies of lecithin dispersions treated with natural surface active substances. The morphologies include multilamellae, rod-shaped assemblies (lecithin + cholesterol) and stacked donuts (lecithin + cholesterol + saponin). The morphology of lecithin liposomes modified by lysolecithin was subsequently examined in detail by Howell et al.[26] and by Inoue et al.[27] Stacked disks and rod-shaped structures were seen abundantly in these cases. More recently, Segrest and others[14,28] showed for stacked disks formed from lecithin and apolipoprotein that apolipoprotein is located in the peripheral region of the disk. In these natural lipid systems, the discussion on the relation between the aggregate morphology and the chemical structure of the components is virtually nonexistent. The present study is the first attempt to establish this relationship through natural and synthetic amphiphiles.

Biological functions in a living cell are closely related to the morphology of organelles. The same can hold true in the synthetic system. The present results may be useful for developing morphology-related functions in artificial molecular assemblies. As advocated by Kuhn,[29] a variety of new functions which are impossible to achieve by a collection of free molecules may be realized on the basis of synthetic molecular assemblies. The morphology control or assembly control will be an important foundation for achieving this goal.

Scheme I

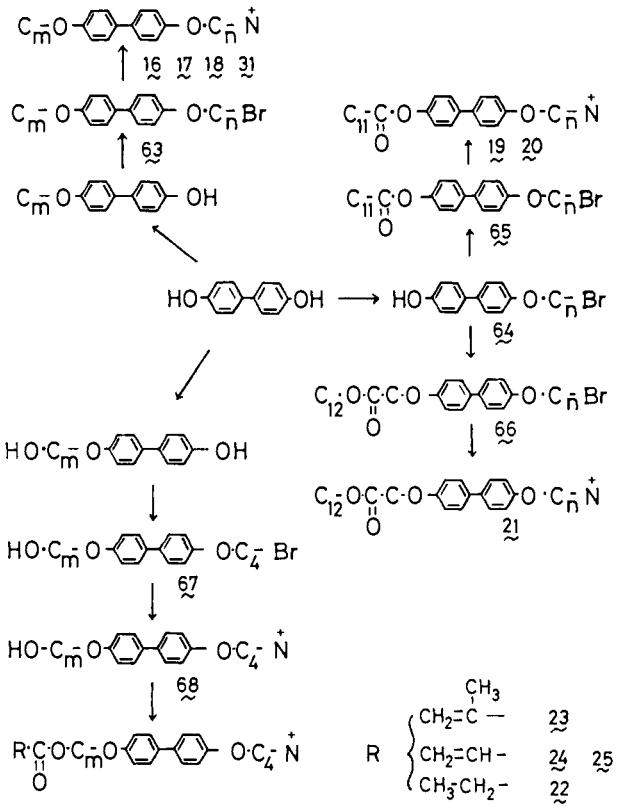

Experimental Section

The structures of the intermediates and the final products were confirmed by thin-layer chromatography, IR and NMR spectroscopies, and elemental analysis. The melting point was measured with a polarizing microscope and the liquid crystalline region is denoted by the arrow.

Amphiphiles with Diphenylazomethine Rigid Segments. The preparations of amphiphiles **1–9** have been described elsewhere.[6] Amphiphiles **10–15** were prepared in similar ways by the coupling of appropriate amine and benzaldehyde components and recrystallized. **10**: colorless powders; mp 130→142 °C. Anal. Calcd for $C_{22}H_{39}N_2Br$: C, 64.20; H, 9.57; N, 6.81. Found: C, 64.03 H, 9.63 N, 6.75. **11**: colorless powders; mp room temperature→223 °C. Anal. Calcd for $C_{26}H_{43}N_2OBr \cdot H_2O$: C, 62.75; H, 9.13; N, 5.63. Found: C, 62.60; H, 9.92; N, 5.56. **12**: colorless powders; mp 168→173 °C. Anal. Calcd for $C_{32}H_{55}N_2OBr$: C, 68.17; H, 9.85; N, 4.97. Found: C, 67.67; H, 10.42; N, 4.86. **13**: colorless plates; mp 197→216 °C. Anal. Calcd for $C_{29}H_{45}N_2O_2Br \cdot {}^1/_2H_2O$: C, 64.41; H, 8.55; N, 5.15. Found: C, 64.37; H, 8.55; N, 5.20. **14**: pale yellow needles; mp 79→103 °C. Anal. Calcd for $C_{32}H_{51}N_2OBr \cdot H_2O$: C, 66.53; H, 9.52; N, 4.85. Found: C, 66.87; H, 9.31; N, 4.93. **15**: colorless plates; mp 60→75 °C. Anal. Calcd for $C_{32}H_{51}N_2O_2Br \cdot 3H_2O$: C, 61.04; H, 9.12; N, 4.45. Found: C, 61.46; H, 8.60; N, 4.52.

Amphiphiles with Biphenyl Rigid Segments. The preparations of **18**, **30**, **32–37** and **39** have been reported.[7,16,18] The preparations of **26–29** and **38** will be published separately.[15,17] The synthetic routes of the other amphiphils in this category are summarized as shown by Scheme I.

Preparations of 16 and 17. In the procedure similar to that for **18**,[7] *p*-(hexyloxy)-*p'*-hydroxybiphenyl (mp 147→155 °C) and *p*-(octyloxy)-*p'*-hydroxybiphenyl (mp 135→148 °C) were allowed to react with 1,4-dibromobutane to give the corresponding bromo derivatives (**63** (m = 6), mp 108–110 °C; **63** (m = 8), mp 90→114 °C), which were then quaternized with trimethylamine. **16**: colorless powders; mp 190→210 °C. Anal. Calcd for $C_{25}H_{38}NO_2Br \cdot {}^3/_2H_2O$: C, 61.09; H, 8.10; N, 2.85.

(25) Bangham, A. D.; Horne, R. W. *J. Mol. Biol.* **1964**, *8*, 660–668.
(26) Howell, J. S.; Fisher, D.; Goodall, A. H.; Verringer, M.; Lucy, J. A. *Biochim. Biophys. Acta* **1973**, *332*, 1–10.
(27) Inoue, K.; Suzuki, K.; Nojima, S. *J. Biochem.* **1977**, *81*, 1097–1106.
(28) Segrest, J. P. *Chem. Phys. Lipids* **1977**, *18*, 7–22.
(29) Kuhn, H. *Ber. Bunsenges. Phys. Chem.* **1976**, *80*, 1209.

Found: C, 61.15; H, 8.20; N, 3.32. **17**: colorless powders; mp 185→195 °C. Anal. Calcd for $C_{27}H_{42}NO_2Br \cdot {}^1/_2H_2O$: C, 64.66; H, 8.64; N, 2.79. Found: C, 64.49; H, 8.66; N, 2.78.

Preparation of 19 and 20. Nineteen millimoles (n = 4, 6.2 g; n = 10, 7.7 g) of p-(ω-bromoalkyloxy)-p'-hydroxybiphenyl **64** (n = 4, mp 137→145 °C; n = 10, mp 120→130 °C) and trimethylamine (40 mmol, 4.0 g) were dissolved in purified dimethylformamide (DMF) and 6.0 g (27 mmol) of dodecanoyl chloride in ether were added dropwise with ice cooling. The mixture was then allowed to react for 2 h at room temperature and poured into a large excess of water. The precipitates were recrystallized from acetone and ethanol: **65** (n = 4), yield 6.5 g (67%), mp 70→110 °C; **65** (n = 10), yield 3.8 g (53%), mp 85→99 °C. The products (n = 4, 5.0 g (10 mmol); n = 10, 1.0 g (1.7 mmol)) were dissolved in benzene, added with excess trimethylamine (27% ethanol solution), and allowed to react for 75 h at room temperature. The precipitates (**19** or **20**) were separated and washed with benzene. **19**: colorless powders; yield 4 g (71%); mp 170→185 °C. Anal. Calcd for $C_{31}H_{48}NO_3Br$: C, 66.18; H, 8.60; N, 2.49. Found: C, 65.81; H, 8.49; N, 2.52. **20**: colorless powders; yield 0.9 g (82%); mp 198→204 °C. Anal. Calcd for $C_{37}H_{60}NO_3Br \cdot H_2O$: C, 67.35; H, 9.30; N, 2.15. Found: C, 67.22; H, 9.25; N, 2.21.

Preparation of 31. **63** (m = 12, n = 10)[7] was refluxed in benzene in the presence of excess (dimethylamino)ethanol to give colorless precipitates of **31**: mp 124→168 °C. Anal. Calcd for $C_{38}H_{64}NO_3Br$: C, 68.86; H, 9.73; N, 2.11. Found: C, 68.28; H, 9.76; N, 2.06.

Preparation of 21. **64** (n = 6) (mp 123→135 °C, 1.3 g (3.7 mmol)) and 4.9 g (1.9 mmol) of dodecyl chloroacetate were dissolved in 50 mL of $CHCl_3$, and 0.3 g (7.5 mmol) of NaOH and 0.2 g (0.77 mmol) of Bu_4N^+OH in 50 mL of water were added. The mixture was stirred for 40 h at 40 °C. The organic layer was dried, the solvent removed, and the residue recrystallized two times from ethanol. **66** (n = 6): pale yellow powders; yield 1.0 g (81%); mp 88→91 °C. The product was quaternized in a way similar to that for **19** and the precipitates were recrystallized from a mixture of benzene, ethanol, and acetone. **21** (n = 6): colorless powders; yield 0.3 g (34%); mp 200→205 °C. Anal. Calcd for $C_{35}H_{56}NO_4Br$: C, 66.25; H 8.83; N, 2.21. Found: C, 66.34; H, 8.72; N, 2.03.

Preparation of 22, 23, 24, and 25. p-(ω-Hydroxyhexyloxy)-p'-hydroxybiphenyl (colorless powders, mp 140→153 °C) (7.0 g, 25 mmol) and 1.0 g (25 mmol) of NaOH were dissolved in ethanol and 15.9 g (75 mmol) of 1,4-dibromobutane in ethanol were added dropwise in 15 min and refluxed for 21 h. The reaction mixture was filtered while warm, the solvent removed, and the residue recrystallized twice from ethanol to give colorless powders. **67** (m = 6): yield 3.8 g (45%); mp 110→133 °C. The product (3.5 g, 8.3 mmol) in 100 mL of benzene and 30 mL of 27% trimethylamine in ethanol were sealed in an ampule and allowed to react for 40 h at 85 °C. The solvents were removed and the residue recrystallized from methanol and ethyl acetate to give colorless powders of **68** (m = 6): yield 2.1 g (48%); mp 180→220 °C. To an acetonitrile solution of 1.5 g (3.6 mmol) of **68** (m = 6), 2.3 g (22 mmol) of triethylamine, and 5 mg of 2,6-di-*tert*-butyl-p-cresol were dropwise added acetonitrile solutions of the acid bromides (7.4 mmol) in 40 min. Stirring was continued for 1–2 h at room temperature. Acetonitrile was removed, and the residues taken up in methylene chloride were washed twice with water. The organic layers were dried, the solvent removed, and the residues recrystallized from $CHCl_3$ and acetone. **22**: colorless powders; yield 0.5 g (30%); mp 155→165 °C. Anal. Calcd for $C_{29}H_{42}NO_4Br \cdot H_2O$: C, 61.48; H, 7.82; N, 2.43. Found: C, 61.85; H, 7.89; N, 2.64. **23**: colorless powders; yield 0.5 g (30%); mp 88→145 °C. Anal. Calcd for $C_{30}H_{42}NO_4Br \cdot H_2O$: C, 61.54; H, 7.83; N, 2.42. Found: C, 61.95; H, 7.90; N, 2.64. **24**: colorless powders; yield 0.5 g (30%); mp 100→145 °C. Anal. Calcd for $C_{29}H_{40}NO_4Br$: C, 63.77; H, 7.38; N, 2.65. Found: C, 63.12; H, 7.70; N, 2.53. **25** was prepared by similar procedures: yellowish powders, mp 85→150 °C.

Amphiphiles with Azobenzene and Azoxybenzene Rigid Segments. The synthetic routes of the azobenzene-containing ammonium amphiphiles are summarized in Scheme II. The preparations of **40–42** and **44–46** will be reported elsewhere.[20,22] The preparation of **47** was described briefly.[18]

Preparation of 43. p-(ω-Hydroxyhexyloxy)acetanilide, mp 70→75 °C (6 g, 24 mmol) in 100 mL of ethanol was added to 10 mL of concentrated hydrochloric acid and refluxed for 5 h. Solvents were removed, and the residue was dissolved in 100 mL of 1:1 aqueous acetone and 10 mL of concentrated hydrochloric acid added. To this mixture were added 50 mL of aqueous $NaNO_2$ (2.5 g, 30 mmol) with stirring in an ice bath. The obtained solution of the diazonium salt was added to a 100-mL aqueous solution of 3.4 g (37 mmol) of phenol, 1.5 g (35 mmol) of NaOH, and 6 g (57 mmol) of Na_2CO_3, and the mixture was stirred for 12 h at room temperature. It was neutralyzed with acetic acid and the yellow precipitates were recrystallized to give yellow powders of **69**: yield

Scheme II

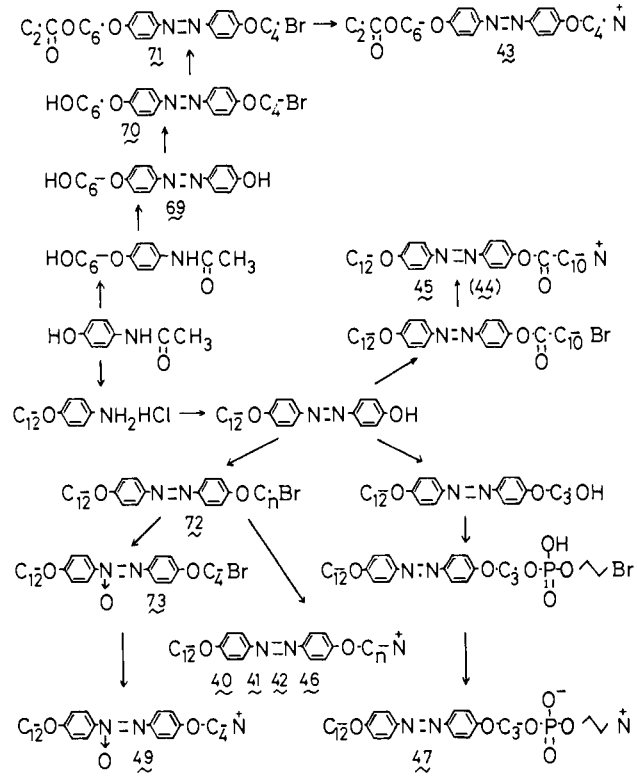

5.0 g (66%), mp 139→149 °C. p-(ω-Hydroxyhexyloxy)-p'-hydroxyazobenzene (**69**) (3.0 g, 95 mmol) and 8.0 g (37 mmol) of 1,4-dibromobutane were allowed to react in refluxing ethanol in the presence of 1 g (15 mmol) of KOH. The yellow precipitates were recrystallized from aqueous ethanol to give 1 g (23%) of **70**: yellow powders; mp 106→114 °C. **70** (2.0 g, 4.5 mmol) was allowed to react with propionyl chloride (0.6 g, 6.5 mmol) in dry benzene in the presence of triethylamine to give ester **71** (mp 85–88 °C) in a 1.5 g (68%) yield. **71** was subsequently quaternized with an ethanol solution of trimethylamine in an ampule and the product recrystallized from ethanol to give **43**: yellow powders; yield 0.86 g (54%); mp 197→219 °C. Anal. Calcd for $C_{28}H_{42}N_3O_4Br \cdot {}^1/_2H_2O$: C, 58.63; H, 7.55; N, 7.33. Found: C, 58.87; H, 7.45; N, 7.23.

Preparation of 49. p-(ω-Bromobutoxy)-p'-(dodecyloxy)azobenzene (**72**) (n = 4) was prepared by diazo coupling of p-(dodecyloxy)aniline and phenol and by the subsequent reaction with 1,4-dibromobutane; mp 96→110 °C. **72** (n = 4) (1.4 g, 2.7 mmol) was suspended in 100 mL of acetic acid which contains 0.8 g of 30% aqueous hydrogen peroxide (7.1 mmol) and stirred for 48 h at 65 °C. The reaction mixture was poured into water and the precipitates were recrystallized to give **73**: pale yellow plates, mp 70→120 °C; yield 0.8 g (56%). **73** was quaternized with triethylamine in ethanol. **49**: pale yellow needles from ethanol and ethyl acetate; yield 0.45 g (51%); mp 220→240 °C. Anal. Calcd for $C_{31}H_{50}N_3O_3Br \cdot H_2O$: C, 61.88; H, 8.54; N, 6.98. Found: C, 61.68; H, 8.49; N, 6.80.

Preparation of 48. Sulfanylic acid (9.5 g, 50 mmol) and 2.0 g (50 mmol) of NaOH were dissolved in 80 mL of water and the mixture was adjusted to pH 4 with acetic acid. To the stirred mixture in an ice bath was added 20 mL of aqueous $NaNO_2$ (4.0 g, 52 mmol). The aqueous diazonium salt obtained was added dropwise to 150 mL of an ethanol solution of 13.7 g (50 mmol) of N-methyl-N-dodecylaniline (bp 135–145 °C (0.01 mm)) in an ice bath. After further stirring for 1 h at room temperature, the mixture was adjusted to pH 10 with aqueous alkali and the precipitates were recrystallized twice from ethanol to give orange plates of **48** in a 16.5 g (55%) yield; mp over 300 °C. Anal. Calcd for $C_{25}H_{36}H_3SO_3Na$: C, 62.37; H, 7.48; N, 8.78. Found: C, 62.82; H, 7.61; N, 8.62.

Amphiphiles with Other Rigid Segments. **50**, **51**, **52** and **62** were synthesized by the stepwise alkylation and quaternization of the dihydroxy starting materials **74**, according to the procedures used for the preparation of **18**[7] (Scheme III). **53–55** were obtained by reduction of **7–9**, respectively, and **56** and **57** were prepared by condensation of aniline derivatives and substituted benzoic acids. The preparations of **58**, **59**, **60**, and **61** will be reported elsewhere.[17,19]

Preparations of 50, 51, 52, and 62. 2,2′-Bis(p-hydroxyphenyl)propane (Bisphenol A; **74a**, X = $-C(CH_3)_2-$) is commerically available. p,p'-

Scheme III

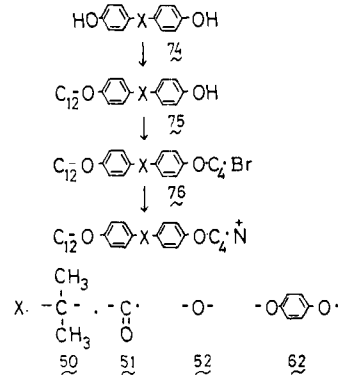

Dihydroxybenzophenone (**74b**, X = –CO–) mp 222–223 °C, was obtained by air oxidation of *p,p'*-dihydroxydiphenylquinomethane.[30] *p,p'*-Dihydroxydiphenyl ether (**74c**, X = –O–), mp 166–167 °C, was obtained by diazotization of *p,p'*-diaminophenyl ether and subsequent hydrolysis.[31] 1,4-Bis(*p*-hydroxyphenyloxy)benzene (**74d**; X = $-OC_6H_4O-$), mp 187–188 °C, was prepared by transmethylation in toluene of the condensation product of *p*-dibromobenzene and hydroquinone monomethyl ether.[32] Monoalkylation of **74** was conducted by reaction of dodecyl bromide in refluxing ethanol in the presence of KOH. Inorganic salts and the didodecyl byproducts were separated, and ethanol was distilled. The residues were extracted with hot hexane when necessary. **75a**: oily product; yield 60%. **75b**: colorless plates from hexane and ethyl acetate, mp 81→89 °C; yield 50%. **75c**: colorless powders from hexane; mp 92–93 °C; yield 60%. **75d**: colorless powders from ethanol; mp 132→150 °C; yield, 50%. **75a–d** were allowed to react with excess 1,4-dibromobutane in refluxing ethanol in the presence of KOH. The precipitates were recrystallized from mixtures of ethanol and benzene. **76a**: colorless wax; yield 73%. **76b**: colorless needles; mp 93–94 °C; yield 63%. **76c**: colorless powders; mp 81–82 °C; yield 63%. **76d**: colorless powders; mp 86→103 °C; yield 69%. **76a–d** were allowed to react with trimethylamine at room temperature for 24–48 h in mixed solvents of benzene, ethanol, and water. After removal of solvents, the residues were recrystallized from ethanol and/or ethyl acetate. **50**: white wax; yield 80%. Anal. Calcd for $C_{34}H_{56}NO_2Br \cdot H_2O$: C, 67.08; H, 9.60; N, 2.30. Found: C, 67.01; H, 9.44; N, 2.35. **51**: colorless powders; mp 75→165 °C; yield 75%. Anal. Calcd for $C_{33}H_{50}NO_3Br \cdot H_2O$: C, 64.63; H, 8.81; N, 2.36. Found: C, 65.52; H, 8.83; N, 2.33. **52**: colorless powders; mp 30→83 °C; yield 81%. Anal. Calcd for $C_{31}H_{50}NO_3Br \cdot H_2O$: C, 63.90; H, 8.99; N, 2.40. Found: C, 64.22; H, 8.96; N, 2.54. **62**: colorless needles; mp 118–120 °C; yield 80%. Anal. Calcd for $C_{37}H_{54}NO_4Br$: C, 67.67; H, 8.29; N, 2.13. Found: C, 67.48; H, 8.40; N, 2.06.

Preparation of 53, 54, and 55. *p'*-(ω-(Trimethylammonio)butyloxy)-*p*-(dodecylbenzylidene)aniline (**8**) (5.5 g, 9.8 mmol) in 100 mL of dry ethanol was added dropwise to a suspension of 0.37 g (10 mmol) of $NaBH_4$ in 20 mL of dry ethanol. After being stirred for 1 day at room temperature, the mixture was refluxed for 2 h and made acidic with hydrobromic acid. The solvents were removed and the residue was reprecipitated from ethanol and ether to give pale yellow powders of **54** in a 5.3 g (85%) yield: mp 185–187 °C. Anal. Calcd for $C_{32}H_{54}N_2OBr_2 \cdot 7H_2O$: C, 50.00; H, 7.03; N, 3.64. Found: C, 49.74; H, 7.03; N, 3.52. **53** and **55** were similarly obtained from **7** and **9**, respectively. **53**: colorless powders; yield 15%; mp 71→145 °C. Anal. Calcd for $C_{28}H_{46}N_2Br_2 \cdot 8H_2O$: C, 47.06; H, 8.74; N, 3.91. Found: C, 47.02; H, 7.03; N, 3.91. **55**: yellow powders; yield 73%; mp 83–85 °C. Anal. Calcd for $C_{38}H_{66}N_2OBr_2 \cdot 6H_2O$: C, 54.67; H, 9.42; N, 3.36. Found: C, 55.11; H, 8.43; N, 3.36.

Preparation of 56. *N,N*-Dimethyl-*p*-phenylenediamine (3.6 g, 26 mmol) and 3.0 g (30 mmol) of triethylamine were dissolved in 50 mL of $CHCl_3$ and 8.5 g (26 mmol) of *p*-(dodecycloxy)benzoyl chloride in $CHCl_3$ were added over 30 min with ice cooling. Stirring was continued for 1 h each at room temperature and at 40 °C. The mixture was washed with aqueous Na_2CO_3 and with water and dried and the solvent removed. The residue was recrystallized from $CHCl_3$: yield 6.5 g (59%); mp 148 °C. The product was allowed to react with excess CH_3Br in an ampule for 50 h at 70 °C, and the precipitates recrystallized from ethanol: colorless needles, yield 5 g (80%); mp 174→190 °C. Anal. Calcd for $C_{28}H_{43}N_2O_2Br \cdot {}^1/_2H_2O$: C, 63.64; H, 8.14; N, 5.30. Found: C, 63.40; H, 8.39; N, 5.33.

Preparation of 57. To a $CHCl_3$ solution of 5.5 g (20 mmol) of *p*-(dodecyloxy)aniline and 3.0 g (30 mmol) of triethylamine was added a $CHCl_3$ solution of 5.8 g (20 mmol) of ω-(bromooxy)benzoyl chloride over 30 min with ice cooling. After further stirring for 1 h at room temperature, the precipitates were recrystallized from $CHCl_3$: colorless needles; yield 7 g (65%); mp 123→137 °C. The product was quaternized in ethanol with trimethylamine: colorless powders from ethanol; yield 5 g (62%); mp 135–137 °C. Anal. Calcd for $C_{32}H_{51}N_2O_3Br$: C, 64.98; H, 8.63; N, 4.74. Found: C, 65.38; H, 8.94; N, 4.70.

Measurements. The surface tension measurement (Wilhelmy method), NMR spectroscopy, and differential scanning calorimetry of amphiphile solutions have been described elsewhere.[6,7] Electron microscopy (Hitachi H-500 electron microscope) was carried out for negatively stained samples and for freeze-fracture replicas. The preparation of negatively stained samples was reported.[6] In the freeze-fracture-replica method, aqueous samples (ca. 10 mM) were placed on a sampling rod and frozen instantaneously by immersing in Freon 22 kept at –160 °C. With use of an Eiko Engineering apparatus (model FD2A), the samples were fractured at –150 °C under 10^{-6} torr and Pt metal and carbon deposited on the fractured surface. The samples were taken out and washed with aqueous glycerol and water.

Fluorescence Spectroscopy. Aqueous solutions (ca. 1×10^{-4} M) of amphiphiles with the biphenyl rigid segment were prepared and their fluorescence spectroscopy was measured with a Hitachi 650-10S instrument. The degree of fluorescence polarization (P) was estimated from eq 1.

$$P = \frac{I_{\parallel} - I_{\parallel\perp}(I_{\perp\parallel}/I_{\perp\perp})}{I_{\parallel} + I_{\parallel\perp}(I_{\perp\parallel}/I_{\perp\perp})} \tag{1}$$

Molecular Weight Measurements. The molecular weight was obtained by a small-angle light-scattering apparatus with the He–Ne laser light sourse (Toyo Soda, LS-8). Clear aqueous solutions of amphiphiles (5 mg/1 mL, ca. 10 mM) obtained by sonication were diluted to 50 mL and filtered with a Teflon filter (Sumitomo Denko Co, Fluoropore, pore size 1 μm). Similarly treated double-distilled water was introduced with a flow rate of 0.6 mL/min and 2.5 mL of the sample solution injected. The scattered light at 5° was detected. The sample concentration was determined by a RI detector (Toyo Soda HLC-802UR or Showa Denko Shodex RI SE-11) which was connected in series. The scattering intensity at a small angle is approximated by

$$R_\theta = Kc\bar{M}_w \tag{2}$$

where R_θ is the Rayleight ratio; M_w is the molecular weight, c is the concentration, and K is the scattering-angle·dependent constant. Since the scattering intensity and the sample concentration are proportional to the observed peak height (H_{LS} and H_{RI}, respectively),

$$H_{RI} = k_1 c \tag{3}$$

$$H_{LS} = k_2 R_\theta \tag{4}$$

Combination of eq 2, 3, and 4 gives

$$\bar{M}_w = \frac{k_1}{k_2 K}\frac{H_{LS}}{H_{RI}} \tag{5}$$

where $(k_1/k_2)K$ was determined as the instrumental constant from reference samples with known molecular weight. The constant was 3.62×10^4 in the present case, as estimated from a series of Toyo Soda monodisperse poly(ethylene oxide): SE-15, $M_w = 1.5 \times 10^5$, $M_w/M_n = 1.04$; SE-30, $M_w = 2.8 \times 10^5$, $M_w/M_n = 1.05$; SE-70, $M_w = 6.6 \times 10^5$, $M_w/M_o = 1.10$; SE-150, $M_w = 1.2 \times 10^6$, $M_w/M_n = 1.12$.

Acknowledgment. The authors are grateful to Professor M. Takayanagi and Professor T. Matsuo for the use of an electron microscope and a surface tension apparatus, respectively. They also appreciate a generous gift of *p,p'*-dihydroxybiphenyl by Sanko Kagaku Co. Capable technical assistance by M. Nagai in the preparation of amphiphiles is appreciated. This work was supported in part by a Grant-in-Aid for Scientific Research, No. 447079.

(30) Gomberg, M.; Snow, H. R. *J. Am. Chem. Soc.* **1925**, *47*, 198–211.
(31) Burckhalter, J. H.; Tendick, F. H.; Jones, E. M.; Holcomb, W. F.; Rawlins, A. L. *J. Am. Chem. Soc.* **1946**, *68*, 1894–1901.
(32) Oesterlin, M., *Monatsh. Chem.* **1931**, *57*, 31–44.